Parametrization in Weather and Climate Models

Hannah Christensen, Oxford University and Laure Zanna, New York University

https://doi.org/10.1093/acrefore/9780190228620.013.826
Published online: 21 December 2022

Summary

Numerical computer models play a key role in Earth science. They are used to make predictions on timescales ranging from short-range weather forecasts to multi-century climate projections. Computer models are also used as tools to understand the past, present, and future climate system, enabling numerical experiments to be carried out to explore physical processes of interest. To understand the behavior of these models, their formulation must be appreciated, including the simplifications and approximations employed in developing the model code.

Foremost among these approximations are the parametrization schemes used to represent subgrid scale physical processes. A useful mathematical formulation of parametrization often involves Reynolds averaging, whereby a flow described by the Navier–Stokes equations is separated into a slow, resolved component and a fast, unresolved component. On performing this decomposition, the component representing the unresolved, fast processes is shown to impact the resolved scale flow: It is this component that a parametrization seeks to represent.

Parametrization schemes encode the understanding of the salient physics needed to describe processes in the atmosphere and ocean and other components of the Earth system, such as land and ice. For example, finding the relationship between the Reynolds stresses and the mean fields of the system is the turbulence closure problem, which is common to both atmospheric and oceanic numerical models. Atmospheric parametrization schemes include those representing radiation, clouds and cloud microphysics, moist convection, gravity waves, and the boundary layer (which encompasses a representation of turbulent mixing). In the ocean, eddy processes must also be parametrized, including stirring and mixing due to both sub-mesoscale and mesoscale eddies. The similarities between the parametrization problem in atmospheric and oceanic models facilitate transfer of knowledge between these two communities, such that promising avenues of research in one community can in principle readily be adapted and adopted by the other.

Keywords: numerical modeling, parametrization, climate models, numerical weather prediction, atmosphere, ocean, turbulent mixing, Reynolds averaging, data-driven

Subjects: Modeling

Introduction

The climate system is characterized by a multitude of phenomena on a wide range of spatial and temporal scales in the ocean and atmosphere (figure 1). Atmospheric processes include cloud microphysics (less than a few centimeters), small-scale turbulence (<1 m), clouds and convective storms (1–20 km), fronts (10–1,000 km), cyclones (1,000 km), and large-scale planetary waves (5,000 km). In the ocean, processes include mixing and internal waves (<1 km), sub-mesoscale to mesoscale eddies (1–100 km), zonal jets (100s km), and basin-scale circulations (1,000s km).

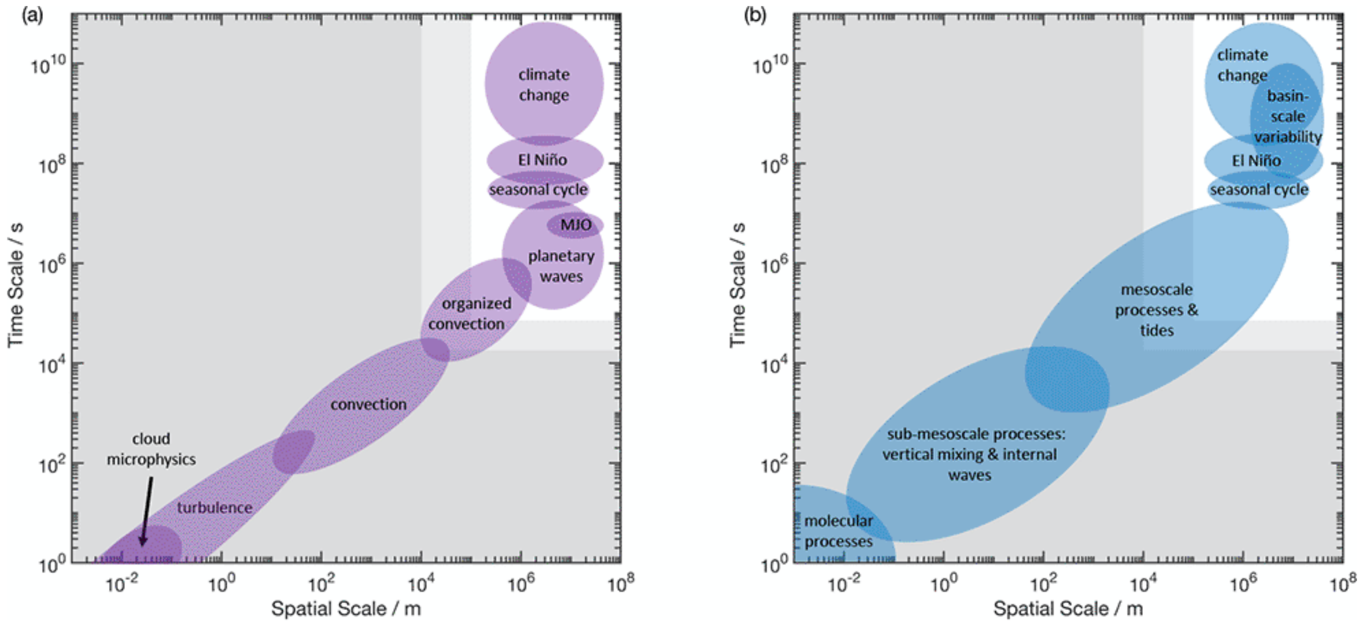

Figure 1. Continuum of scales: schematic of typical length scales and spatial scales for (a) the atmosphere and (b) the ocean. The shaded darker gray region indicates scales unresolved at typical numerical weather prediction model resolution (10 km spatial scale, 5 min time step). At a typical climate model resolution (100 km spatial scale, 20 min time step), the pale gray shaded regions are also unresolved.

Sources: Adapted from UCAR COMET Program <https://www.comet.ucar.edu/> and Dickey (2001).

The continuous interaction between these phenomena across scales governs atmosphere, ocean, and climate dynamics. For example, in the atmosphere, the formation of mid-latitude cyclones enhances temperature gradients leading to the generation of fronts, which support convective storms (e.g., Hobbs et al., 1980). In the ocean, sub-mesoscale eddies generated by large-scale atmospheric forced mixed layer instabilities are important for initiating and sustaining the mesoscale eddy field, with impacts on the seasonality of ocean dynamics (Sasaki et al., 2014). In the tropics, during an oceanic El Niño event, anomalous localized atmospheric winds trigger the propagation of planetary-scale waves in the ocean and the spreading of warm surface temperatures, which then modify atmospheric moist convection, the Walker circulation, and precipitation patterns (e.g., Rasmusson & Wallace, 1983).

With regard to simulating weather and climate, resolving all scales of motion in the ocean and atmosphere is not feasible (Balaji, 2021). Climate simulators are truncated versions of the equations of motion for the ocean and atmosphere systems. These simulators must, therefore, parametrize processes below the scales resolved—breaking the continuum of scales in the ocean and atmosphere (see figure 1).

Parametrization is designed to represent the effect of unresolved, subgrid-scale processes on the resolved scale state. Subgrid-scale processes are separated into a number of conceptual physical phenomena, such as atmospheric convective clouds or ocean mesoscale eddies, each of which is encoded by a separate parametrization scheme. The main atmospheric and oceanic parametrizations are illustrated in Figure 2. These parametrization schemes are local in horizontal space, allowing for efficient parallelization of the model code, and are designed to represent subgrid processes occurring within a single vertical column of the atmosphere or ocean. These parametrizations of subgrid processes are often derived from first principles (e.g., Arakawa & Schubert, 1974) or from statistics based on a data-driven approach (Monin & Obukhov, 1954). A combination of both these approaches is also possible (Schneider, Teixeira, et al., 2017).

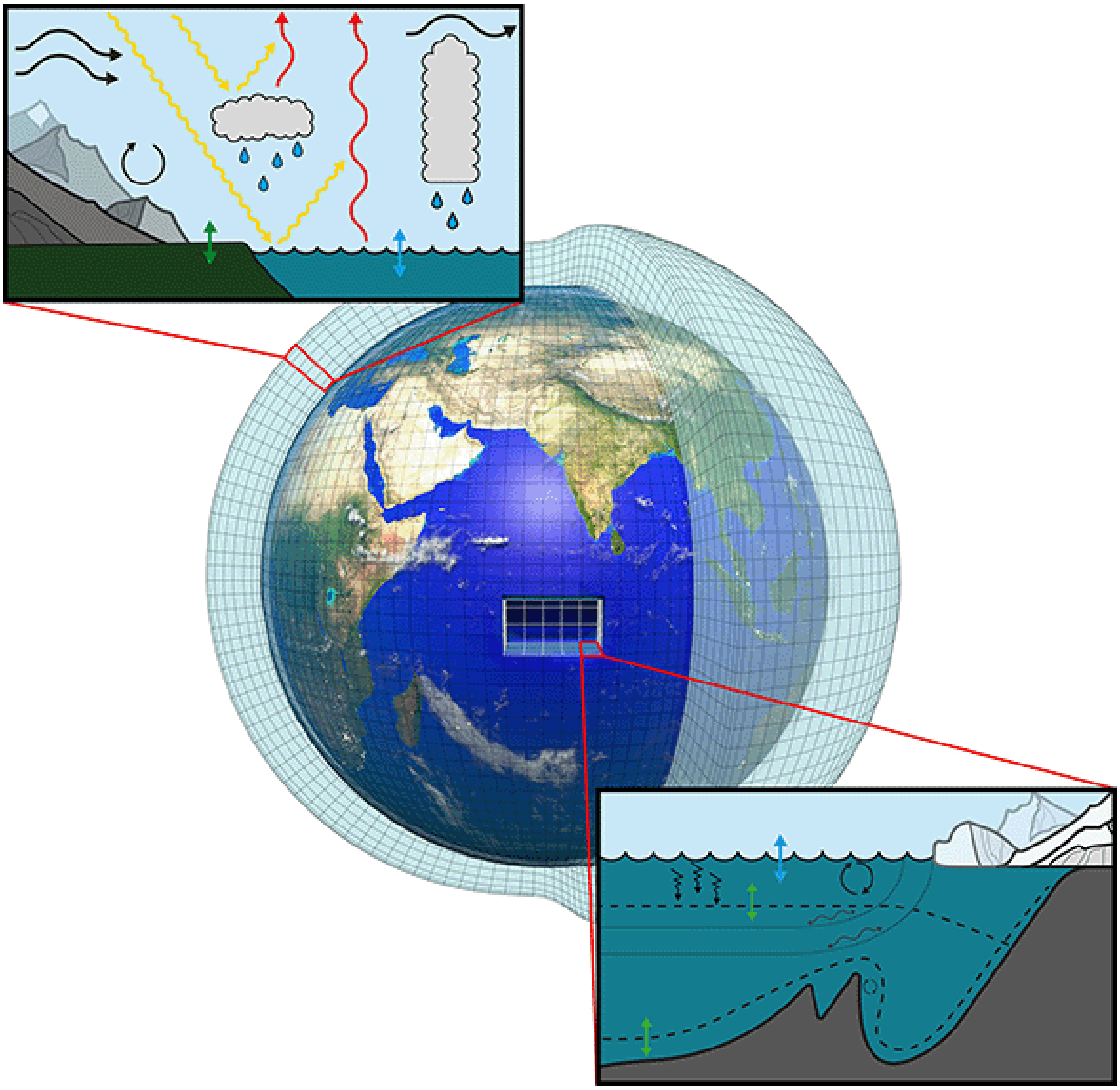

Figure 2. Atmospheric and oceanic parametrization schemes. Within an atmospheric column, typical parametrization schemes include moist convection, clouds and cloud microphysics, radiation, turbulence, turbulent exchange with the land and ocean, and both orographic and non-orographic gravity wave drag. Within an oceanic column, typical parametrization schemes include vertical diffusion, sub-mesoscale and mesoscale eddies, turbulent exchange with the atmosphere, and cross-thermocline transports.

Source: Authors

Even simple approaches to parametrization can be effective. For example, moist convective adjustment schemes represent convection as a process that acts to remove instability from the atmosphere. In such a scheme, the moist convection parametrization simply relaxes temperature and humidity fields toward a prescribed vertical profile (Betts, 1986; Manabe et al., 1965). Note that in addition to representing an important process, the moist convection parametrization is necessary for the model simulations to remain stable. Similarly, in the ocean, convective adjustment instantaneously mixes density (temperature and salinity) within the water column (Klinger et al., 1996). More sophisticated (and more common) approaches build a conceptual model of the small-scale processes in order to estimate the feedback onto the large scale. For example, an "entraining plume" model forms a core component of atmospheric convective cloud mass-flux parametrizations (e.g., Arakawa & Schubert, 1974; Bechtold et al., 2001; Yano, 2014).

At the core of the parametrization problem is the fact that the prognostic variables on the resolved scale are unable to fully constrain the subgrid-scale motions (Figure 3). In light of this caveat, traditional methods for parametrization are designed to represent the mean effect of the small-scale processes given the large-scale state. If a scale separation existed, and provided the grid box were large enough to contain many small-scale motions, the mean of all possible small-scale processes would be a good estimate of the true subgrid tendency (as assumed in, e.g., Arakawa & Schubert, 1974). The lack of scale separation in both the atmosphere and the ocean means that this approach is one source of error in climate simulators (Berner et al., 2017; Dorrestijn et al., 2013).

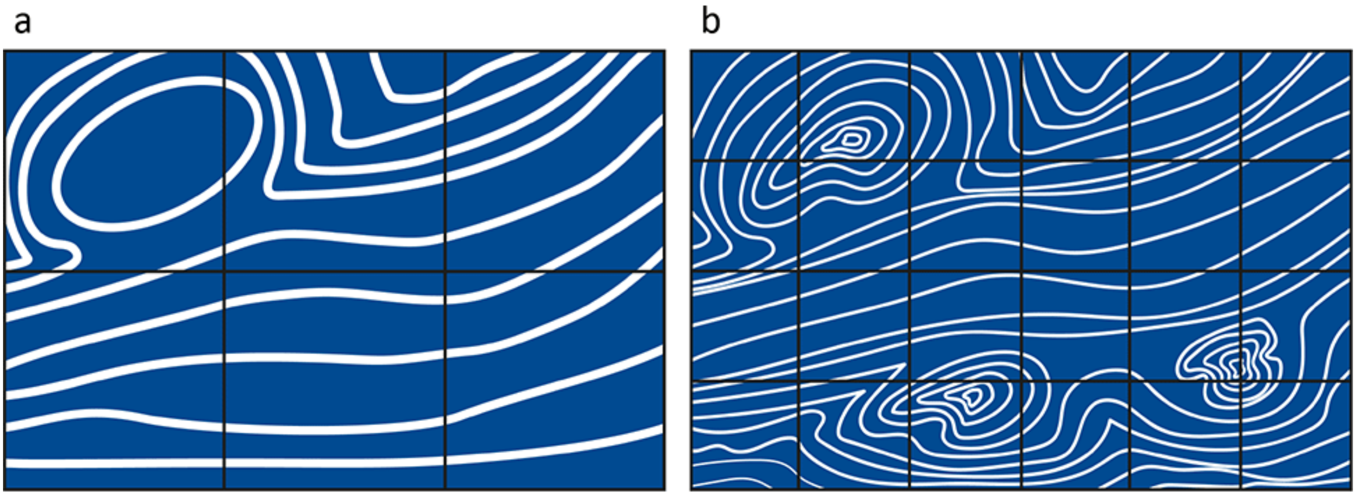

Figure 3. Streamlines representing an oceanic flow field in a typical (a) low-resolution model and (b) high-resolution model. The model grid is schematically represented as black lines. The low-resolution model is not simply a smoothed version of the high-resolution model. The poor representation of sub-grid and partially resolved eddies degrades the large-scale state of the low-resolution model.

Source: Authors

Many errors (biases) in climate models can be traced to parameterizations. For example, biases in atmospheric jet latitude and orientation have been traced to the representation of orographic drag in climate models (van Niekerk et al., 2017). However, in general it can be difficult to trace model errors to their source. Geographically, small-scale errors can rapidly amplify and cascade to larger scales, impacting remote regions as illustrated by these examples. Within the model, the different parametrization schemes interact with each other, with compensating errors from different parametrization schemes further complicating the picture (e.g., Martin et al., 2010). Numerical models are used at a wide range of resolutions, from the 250-km grid boxes used in paleoclimate models (e.g., Sueyoshi et al., 2013) to 50-km atmospheric grid boxes used for high-resolution climate simulations in Coupled Model Intercomparison Project Phase 6 (CMIP6; e.g., Haarsma et al., 2016) and sometimes finer for the ocean (e.g., Griffies et al., 2015). Global weather forecasting models can reach resolutions of order 10 km in the atmosphere (Bauer et al., 2015). Many processes are unresolved and must be parametrized in both weather and climate models, as shown in Figure 1. This puts great demands on parametrization schemes because the same parametrizations are often used across the whole spectrum of model resolutions. Some atmospheric parametrization schemes are virtually unchanged as resolution changes, including radiation or cloud microphysics (Bauer et al., 2015). However, others, such as moist convection or boundary layer processes, are scale dependent and behave differently across different model resolutions (Han et al., 2017; Holloway et al., 2014), depending on the relative length scales of the grid resolution and the process of interest (Wyngaard, 2004). It is possible to design such schemes to be scale-aware, such that they perform well across different resolutions. This is usually achieved through including resolution-dependent parameters, such as subgrid-scale dissipation in ocean and atmosphere models (Smagorinsky, 1963). Scale-aware parametrizations are in demand in the latest generation of ocean climate models (Bachman et al., 2017) with increased horizontal resolution. This is particularly the case for models with an unstructured grid and variable meshes, in which the resolution varies as a function of location, offering considerable challenges for implementation (Caldwell et al., 2019; Wang et al., 2014).

To conclude this introduction, note that high-resolution atmospheric models used for regional weather prediction (Schalkwijk et al., 2015) and process understanding (Stevens et al., 2020), and the “digital twins” used for climate policy development (Bauer et al., 2021), can be used at ultra-high resolutions of hundreds of meters through to a few kilometers. Yet even at these ultra-high resolutions, a range of processes must still be parametrized, including turbulence, shallow convection, radiation, and cloud microphysics (see figure 1): Weather and climate models will always include subgrid processes that need to be parametrized.

From Physical Equations to Numerical Models: Resolved Scale Dynamics

Constructing a climate model involves solving partial differential equations on a discrete (quasi-) regular grid in space, and at discrete points in time, on a sphere. A parametrization scheme represents the impact of unresolved processes in space and time on the resolved scale flow: This is also achieved in a discrete rather than in a continuous way by mapping the discretized grid-point fields forward in time. To understand how to design a parametrization scheme, it is necessary to understand what a grid-point field represents. The three main frameworks for solving the dynamical equations of motion are therefore considered in turn.

Finite volume models predict the integrated value of a variable over the volume of the grid cell (Machenhauer et al., 2009). Such models make use of the divergence theorem to estimate surface fluxes across the cell surfaces and therefore conserve energy, mass, and momentum (figure 4). Finite volume models therefore explicitly represent the grid-box average of the prognostic variables at a particular time. In contrast, *finite difference* or grid-point models define a spatial grid on which the equations of motion are solved (e.g., the Met Office Unified Model Global Atmosphere component; Walters et al., 2019). This gives the value of the prognostic variables at those points (see figure 4). A key benefit of this approach is its flexibility, allowing for both limited-area and global models, and also enabling resolution to vary across the model domain. *Spectral models* represent the solution to the equations of motion as a sum over a set of orthogonal spectral basis functions (e.g., the atmospheric component of EC-Earth3; Döscher et al., 2021) (see figure 4). The sum is truncated to retain only the leading order wavenumbers in both meridional and zonal directions. The equations are numerically integrated to propagate the coefficients in the summation forward in time. Subgrid parametrized processes must be represented in physical space, necessitating a transform between spectral and grid-point space at every time step. Note that finite element methods, which are occasionally used in atmosphere–ocean modeling, are analogous to spectral models in that they represent climatological fields as a sum over basis functions (e.g., the Finite Element Sea Ice-Ocean Model, Wang et al., 2014). Whereas both finite difference and spectral models represent the value of prognostic variables at a specific point in both space and time, a model with a particular resolution can only represent features with scales greater than four to eight times the grid increment (Abdalla et al., 2013). The grid-point fields are therefore implicitly smoothed compared to the "truth." A grid-point field from such a model must therefore also represent spatial averages in some sense.

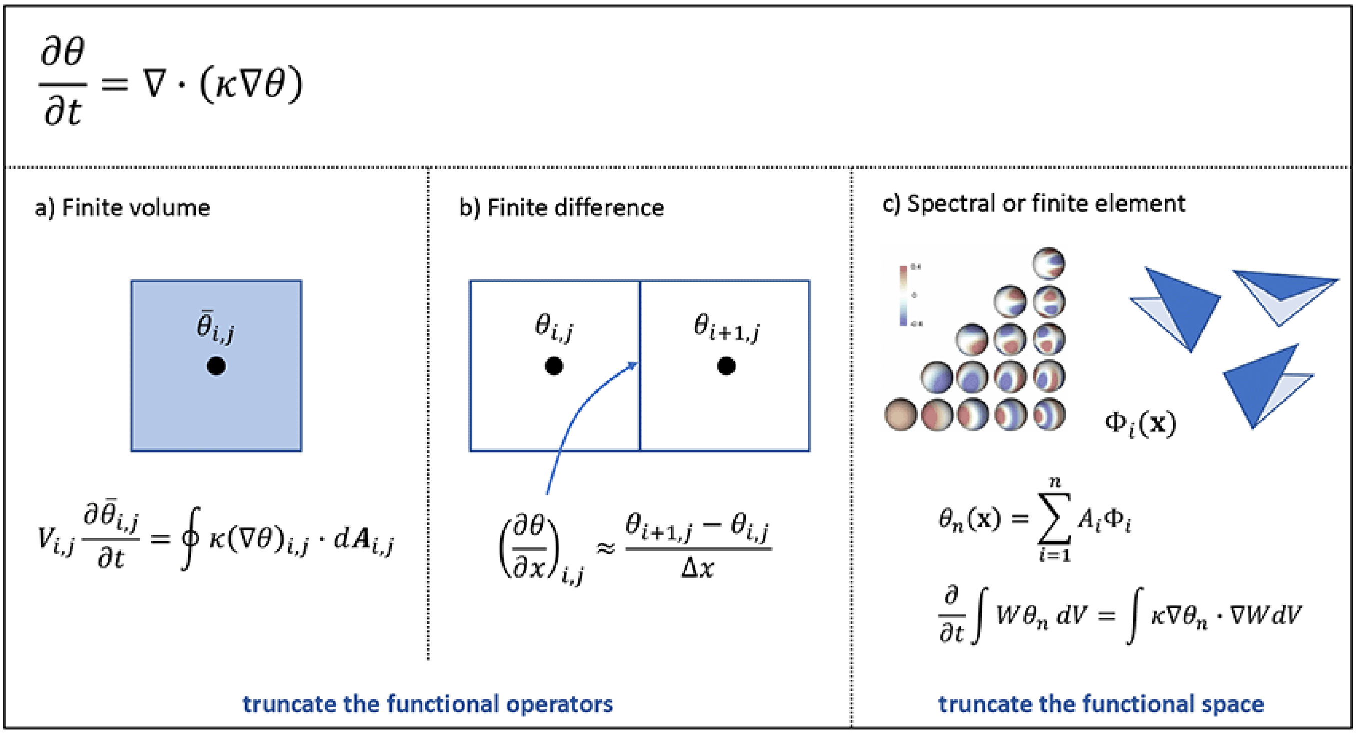

Figure 4. Schematic of three different approaches to discretize the Navier–Stokes equations of motion in weather and climate models. Consider discretizing the diffusion equation. (a) The finite volume approach makes use of the divergence theorem to predict the value of variable θ integrated over the grid box. (b) The finite difference approach represents the variable θ at discrete points in space. (c) Spectral and finite element methods represent the variable θ using a sum over a set of basic functions, where W is a test function.

Source: Authors

Integrating in time propagates the prognostic fields forward from t to $t + \delta t$. A parametrization scheme is thought of within this framework, as providing the subgrid contribution needed to map the resolved scale fields forward from one timestep to the next. Although the resolved field in a finite volume model unambiguously represents an instantaneous value, it is not clear whether a finite difference or spectral model truly represents an instantaneous field at each timestep because the arguments used to justify thinking in terms of a spatial filtering can also be used to justify a temporal average. However, although spatial averaging is commonly used to derive parametrizations and to subsequently couple parametrization schemes to the resolved scale dynamics, considering the implications of temporal averaging is rare (Khairoutdinov et al., 2005; Tang et al., 2017).

From Physical Equations to Numerical Models: Subgrid Physics

Before discussing specific examples of parametrization schemes in the atmosphere and ocean, this section introduces the mathematical ideas needed to understand the parametrization problem. The key parametrizations required by climate models are then outlined in the sections on "Atmospheric Parametrizations" and "Ocean Parametrizations," before addressing one in more detail: this article focuses on the turbulent boundary layer (BL) as an important unresolved process common to atmosphere and ocean models. Furthermore, turbulent processes must be parametrized regardless of the chosen resolution of the model, whether a 100-km resolution climate model or a 100-m resolution large eddy simulation. For a comprehensive review of atmospheric parametrization, see Stensrud (2007).

Reynolds Averaging

The essence of parametrization lies in the separation of scales. The separation of scales can be performed in many ways.

Reynolds averaging as a common decomposition in turbulence theory is reviewed here. The Reynolds decomposition can be written as

$$a = \overline{a} + \overline{a'}, \tag{1}$$

where a is a variable of interest, the overbar represents the average of a, and the prime represents deviations/fluctuations from this average. By definition,

$$\overline{a'} = 0, \tag{2}$$

and for two arbitrary variables, this gives

$$ab = \overline{ab} + \overline{a'b'}. \tag{3}$$

The average is usually taken over an ensemble of realizations, in time or in space. For the development of parameterizations, Reynolds averaging allows the flow to be separated into a fast (small-scale) and slow (large-scale) component. The fast component is generally viewed as the fluctuations due to turbulent eddies which impact the slowly varying and large-scale component of the flow. In parametrization development, it is typical to use a temporal average. However, note that the decomposition also applies if the averaging was carried out in space, as outlined in the section on "From Physical Equations to Numerical Models: Resolved Scale Dynamics." Whereas here averaging in time is considered, because this is the usual theoretical approach used in Reynolds averaging, in the Appendix, Reynolds averaging in space is discussed, with a particular view to deriving data-driven parametrization schemes.

As an example of the application of this approach, consider the horizontal momentum equations for the turbulent BL in the ocean or atmosphere, neglecting forcing and dissipation (for simplicity):

$$\frac{Du}{Dt} = \frac{\partial u}{\partial t} + u\frac{\partial u}{\partial x} + v\frac{\partial u}{\partial y} + w\frac{\partial u}{\partial z} = -\frac{1}{\rho_0}\frac{\partial p}{\partial x} + fv \tag{4}$$

$$\frac{Dv}{Dt} = \frac{\partial v}{\partial t} + u\frac{\partial v}{\partial x} + v\frac{\partial v}{\partial y} + w\frac{\partial v}{\partial z} = -\frac{1}{\rho_0}\frac{\partial p}{\partial y} + fu. \tag{5}$$

The three-dimensional velocity and its components are $\mathbf{u} = (u, v, w)$, $\frac{D}{Dt}$ is the material (Lagrangian) derivative, $\frac{\partial}{\partial t}$ is the local (Eulerian) derivative, p is the pressure, f is the Coriolis parameter, and ρ_0 is the reference density.

Substituting the Reynolds decomposition (Equations 1–3) into the momentum equations (Equations 4 and 5), using the continuity equation, and performing an average with respect to time results in the following equations for the slowly evolving flow:

$$\frac{\overline{D}\overline{u}}{Dt} = -\frac{1}{\rho}\frac{\partial \overline{p}}{\partial x} + f\overline{v} - \left[\frac{\partial\left(\overline{u'u'}\right)}{\partial x} + \frac{\partial\left(\overline{u'v'}\right)}{\partial y} + \frac{\partial\left(\overline{u'w'}\right)}{\partial z}\right] = -\frac{1}{\rho_0}\frac{\partial \overline{p}}{\partial x} + f\overline{v} - S_x \tag{6}$$

$$\frac{\overline{D}\overline{v}}{Dt} = -\frac{1}{\rho}\frac{\partial \overline{p}}{\partial x} + f\overline{u} - \left[\frac{\partial\left(\overline{u'v'}\right)}{\partial x} + \frac{\partial\left(\overline{v'v'}\right)}{\partial y} + \frac{\partial\left(\overline{v'w'}\right)}{\partial z}\right] = -\frac{1}{\rho_0}\frac{\partial \overline{p}}{\partial x} + f\overline{u} - S_y, \tag{7}$$

where the overbar on the material derivative is defined as

$$\frac{\overline{D}}{Dt} = \frac{\partial}{\partial t} + \overline{u}\frac{\partial}{\partial x} + \overline{v}\frac{\partial}{\partial y} + \overline{w}\frac{\partial}{\partial z}.$$

The terms in the square brackets on the right-hand side of Equations (6) and (7), also denoted as S_x and S_y, represent the influence of the turbulent eddies on the mean flow and are the divergence of velocity flux terms, also known as the Reynolds stresses (there are three additional terms in the vertical momentum equation). Performing a Reynolds decomposition on other equations yields similar terms—for example, terms arising from the temperature equation represent the flux of heat within the ocean and/or atmosphere. Finding the relationship between the Reynolds stresses and the mean fields of the system is the turbulence closure problem.

Atmospheric Parametrizations

The formalism of the Reynolds decomposition provides a clear justification of the need for parametrization. It can also be used as a basis for certain parametrizations, such as turbulent fluxes. However, for the three atmospheric parametrization schemes outlined in this section, alternative theoretical or conceptual models have proved useful.

Radiation

Solar radiation is the principal source of energy for the climate system. Differential heating of the atmosphere is responsible for large- and mesoscale atmospheric circulations, including the Hadley circulation, mid-latitude westerlies, monsoon systems, convection, and coastal systems (Warner, 2011). A radiation parametrization must provide an estimate of the total radiative surface flux, for surface energy balance calculations, as well as the vertical and horizontal distribution of radiative heating and cooling rates (Stephens, 1984). The scheme must account for radiative absorption and scattering by trace gases including water vapor, carbon dioxide, and ozone (e.g., Cagnazzo et al., 2007; Iacono et al., 2000), as well as the interaction of radiation with cloud (e.g., Morcrette, Barker, et al., 2008; Shonk et al., 2010). Radiative transfer is well understood, but performing the calculation with high accuracy—that is, with fine spectral resolution and at high frequency in space and time—is very expensive computationally (Morcrette, Mozdzynski, & Leutbecher, 2008; Pincus et al., 2003). The chosen parametrization scheme is therefore a balance between numerical accuracy and cost (Pincus & Stevens, 2013). A common approach to reducing computational cost is to call the scheme infrequently in space and time. Cost can be further reduced through sampling the cloud state and spectral interval (Morcrette, Mozdzynski, & Leutbecher, 2008; Pincus et al., 2003).

Cloud Microphysics

Another process that must be parametrized in all atmospheric models is cloud microphysics. This covers physics that occurs on the scale of cloud droplets, including processes (e.g., condensation, accretion, and deposition) that transfer water between different species, such as vapor, cloud droplets, rain droplets, and ice particles (Lin et al., 1983; Murakami, 1990). To calculate the rate of these various processes, the number concentrations and sizes (and ideally, shapes) corresponding to the different species are required. *Bin models* approach the problem by dividing the range of particle sizes into bins for each species and tracking the number of particles in each bin (Khain et al., 2015). Although accurate, this is computationally expensive, so most atmospheric models use a computationally efficient *bulk model*, which assumes a distribution of particle size for each species. A key output of both bin and bulk cloud microphysics parametrizations is the spatiotemporal distribution of precipitation type and rate (Morrison et al., 2009). Cloud microphysics is also of central importance for climate prediction because of uncertainties in cloud feedbacks (Tan et al., 2016; Zelinka et al., 2020) and the interaction of clouds with natural or anthropogenic aerosol (Gettelman, Hannay, et al., 2019).

Moist Convection

To resolve atmospheric moist convection, models must have a resolution of order 100 m (Bryan et al., 2003), although atmospheric models with resolutions of a few kilometers are often referred to as "convection permitting" or "storm resolving" models when run with the convection scheme deactivated (Holloway et al., 2012; Stevens et al., 2019). Given these requirements, global weather (≈10 km resolution) and climate models both require moist convection to be parametrized: The resultant scheme is often referred to as the "convection" scheme. Moist convection must be accurately represented both for its impact on extreme weather (Bassil, 2014) and for its contribution to driving the global circulation (Donner et al., 2001). Climate models are very sensitive to the chosen convection parametrization (Knight et al., 2007), introducing uncertainties into simulations of future climate. A wide range of convection parametrization schemes have been developed. Although some employ a simple relaxation approach (e.g., Betts, 1986; Manabe et al., 1965), most modern weather and climate models employ a mass-flux scheme (e.g., Arakawa & Schubert, 1974; Gregory & Rowntree, 1990; Kain, 2004; Tiedtke, 1989). In its purest form, this approach assumes a convection parametrization can be formulated in terms of the flux of mass alone—that is, without also considering the in-cloud vertical velocity or convective area fraction. The mass flux at the cloud base can be determined by assuming convective quasi-equilibrium—that is, that moist convection responds to counteract large-scale forcing over a short enough timescale (Arakawa & Schubert, 1974; Bechtold et al., 2014). The mass flux feeds one or more idealized convective clouds called "entraining plumes": As a plume rises from cloud base, it becomes diluted through entrainment of dry environmental air (e.g., Arakawa & Schubert, 1974; Bechtold et al., 2001; Yano, 2014). In a bulk model, it is assumed that a single plume can be used to represent the effect of all convective clouds within the grid box, whereas in a spectral model, convective clouds are grouped together according to their characteristics and modeled using a separate plume for each group (Plant, 2010). Key impacts of the convection scheme include the restabilization of the atmospheric column, the transport of moisture, and convective precipitation. For a comprehensive review of atmospheric moist convection parametrization, see Plant and Yano (2016).

Ocean Parametrizations

The development of ocean parametrizations has been led by a range of semi-empirical models justifying the impact of the subgrid scales on the large scale. In this section, examples of ocean parametrizations and the underlying assumptions employed to derive the parametrizations are described.

Air–Sea Fluxes

Air–sea fluxes of momentum and heat at the interface between the ocean and atmosphere are critical for driving ocean transport on all scales. These fluxes, which have a vast range of spatial and temporal scales, are commonly parametrized using a bulk flux formulation with empirical coefficients. Whereas momentum coefficients can include a dependency on the wind speed, sensible and latent heat coefficients are empirically based on eddy-correlation fluxes compiled from very few observational field experiments (Cronin et al., 2019). The influence of these fluxes can lead to uncertainty in projection of ocean heat uptake and associated thermosteric sea level rise (Huber & Zanna, 2017).

Momentum Transport

In ocean models, turbulent (eddy) processes are assumed to redistribute momentum similarly to molecular diffusion but on a much larger scale. In other words, subgrid fluxes are assumed to be on average down-gradient and act to homogenize the resolved momentum field. The eddy viscosity coefficient modulates the strength of the mixing. Such eddy down-gradient parametrizations improve the numerical stability of ocean models and dissipate enstrophy at the grid scale. The parametrizations of Smagorinsky (1963) and Leith (1968) build upon the eddy viscosity concept by constructing the eddy viscosity coefficient to have a functional dependence on the resolved flow and are widely used in climate models.

Mesoscale and Sub-Mesoscale Eddies

The main mesoscale eddy parametrization used in climate models is concerned with adiabatic buoyancy fluxes in the ocean interior, below the mixed layer. The primary parametrization of Gent and McWilliams (1990) and Tréguier et al. (2012) mimics baroclinic instability by mesoscale eddies via the flattening of isopycnals. Eddies are assumed to reduce stratification by extracting available potential energy from the resolved flow. Redi (1982) also provides a common tracer parametrization that assumes eddies mix *along* isopycnals, rather than horizontally, and can be used in conjunction with the parametrization of Gent and McWilliams (1990).

Sub-mesoscales, with scales of 1–10 km, are important within the mixed layer. The parametrizations of sub-mesoscale processes currently tackle the restratification in the upper ocean caused by diabatic processes (e.g., Fox-Kemper et al., 2008) and are implemented in a range of climate models (e.g., Dunne et al., 2020).

Turbulent Vertical Mixing in Oceanic and Atmospheric Boundary Layers

The boundary layer (BL) is defined as the layer of a fluid that experiences the effect of a boundary. This section discusses in more detail the parametrization of the two most common BLs: the atmospheric planetary BL, which is the part of the troposphere directly influenced by the Earth's surface—namely the land or ocean—and the surface BL of the ocean, which is directly influenced by the presence of the atmosphere above. The depth of these layers will be determined, in part, by mixing generated from the surface buoyancy and momentum fluxes, resulting in thicknesses that can range from hundreds of meters to a few kilometers in the atmosphere (Seidel et al., 2010; Von Engeln & Teixeira, 2013) and from tens to hundreds of meters in the ocean (Carton et al., 2008), with changes on timescales of a matter of hours.

The atmospheric and oceanic BLs are shown schematically in figure 5. A well-mixed atmospheric BL includes the viscous and inertial sublayers and the mixed layer (Moeng, 2016). The viscous (or roughness) sublayer is influenced by individual roughness elements such as buildings and vegetation. The viscous and inertial sublayers together make up the surface layer. This layer is characterized by an approximate balance between the pressure gradient, Coriolis, and friction forces: the Ekman balance. Embedded within the surface layer are eddies that transport mass and momentum from the surface aloft. Above the surface layer is the mixed layer. This layer is convectively active. The structure of the oceanic BL mirrors that of the atmosphere, including both the surface Ekman layer and the mixed layer (see figure 5). The oceanic BL is bounded by the thermocline, a region of strong vertical temperature gradients.

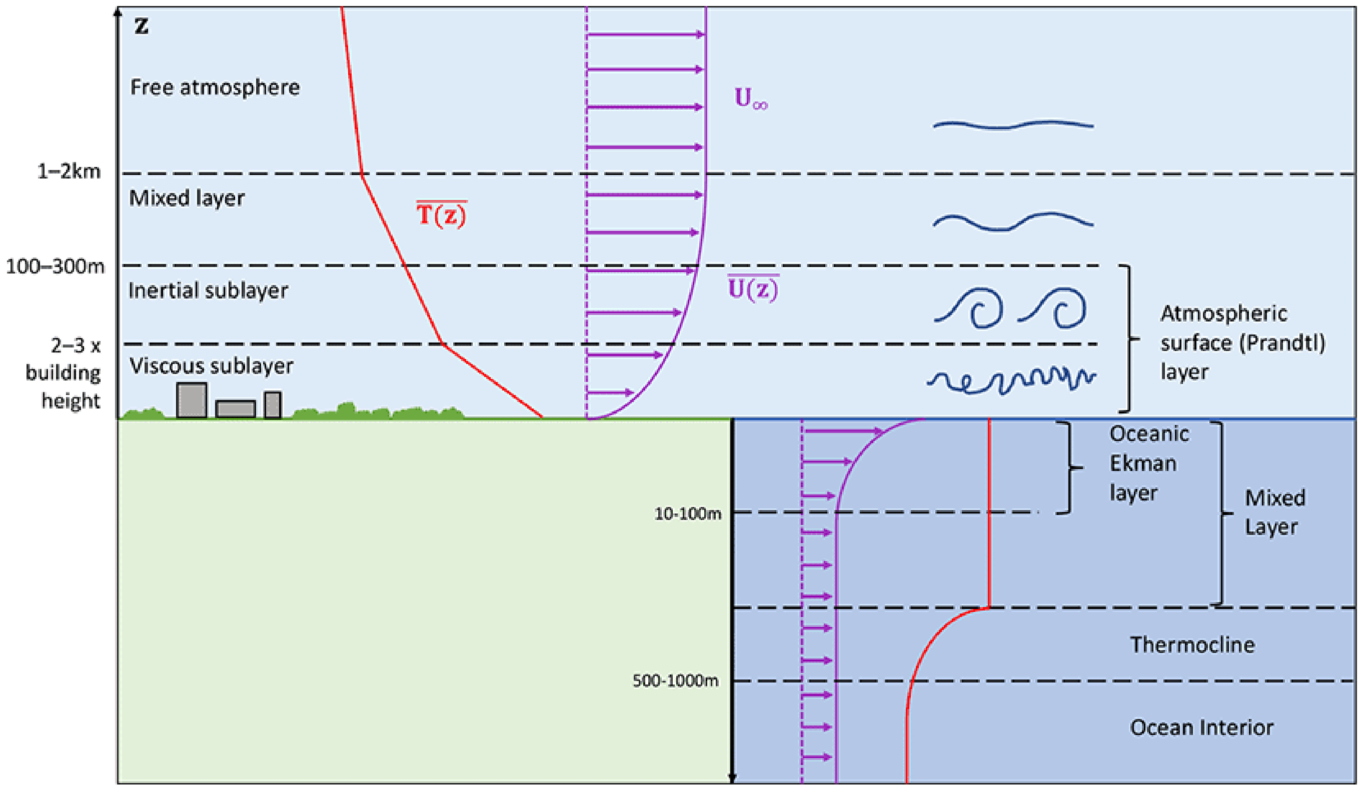

Figure 5. Schematic of vertical mixing in the atmospheric and oceanic boundary layers. Typical mean temperature profiles are shown in red, and wind or ocean current profiles are shown in purple. The schematic shows a well-mixed atmospheric boundary layer, most typical of daytime conditions over land.

Source: Authors

Whereas the well-mixed atmospheric BL shown in figure 5 is common over land during the day, at night it is common for a stable atmospheric BL to form (Steeneveld, 2014). In this situation, long-wave radiative cooling leads to a land surface that is colder than the atmosphere above. This results in potential temperature increasing with height, and stable stratification. Atmospheric BLs can also include clouds, with the BL either topped by a layer of stratocumulus or associated with individual, randomly distributed cumulus clouds (Moeng, 2016). To simplify the discussion, neither stable nor cloudy atmospheric BLs are discussed further in this section.

Climate models are able to reproduce the mean observed atmospheric BL depth but struggle to capture the observed diurnal and seasonal variations (Davy, 2018), likely due to errors in the BL parametrization (Holtslag et al., 2013). In particular, it is known that the different approximations used when parametrizing *turbulence* within the BL scheme can have significant impacts on the simulated climate in numerical models (Christensen & Driver, 2021; Davy & Esau, 2014; Garratt, 1993), including the sensitivity of the model to changes in external forcing (Davy & Esau, 2014, 2016). This sensitivity has led to systematic intercomparison studies such as the GEWEX Atmospheric Boundary Layer Study (Holtslag, 2006).

Mixing in the BL is driven by a combination of surface buoyancy and momentum fluxes. The Obukhov length, L, is used to characterize the ratio of turbulent kinetic energy production from buoyancy compared to shear for different heights above the ground, z, and is a key ingredient to estimate turbulent fluxes. Within the surface layer, Monin–Obukhov similarity theory is used to model vertical variations in the mean flow. If the Obukhov stability parameter z/L is positive, the layer is stably stratified, whereas negative values indicate unstable stratification (Foken, 2006; Monin & Obukhov, 1954). Small-scale turbulent eddies interact with larger scale (but still unresolved) organized features such as thermals and convective rolls (see figure 5; Etling & Brown, 1993), with large impacts on unresolved fluxes. The interaction of mixing with different scales, against a stably or unstably stratified background, leads to very different characteristics of mixing: These different regimes should be represented within the BL parametrization (Degrazia et al., 2000).

There are two main types of closures in turbulence, local and nonlocal, and both have been used for parametrizing BL mixing (e.g., Holtslag & Boville, 1993; Xie et al., 2012). In local closures, the vertical flux of a scalar, $\overline{w'C'}$, is parametrized using variables and/or gradients of known variables at that same point, where C' is the scalar of interest (e.g., temperature and humidity). This leads to an expression analogous to molecular diffusion. In contrast, nonlocal closures rely on values and/or gradients of known variables at different locations in space, typically spanning the vertical column. This is more closely in line with advective processes and often results in more accurate closures for well-mixed BLs. The accuracy of the closure can also be improved by increasing its *order*. A first-order scheme includes prognostic equations for the state variables with the second-order terms (i.e., covariances) parametrized, whereas a second-order scheme also explicitly predicts the evolution of the covariances with the triple correlations parametrized, etc. (Bogenschutz et al., 2013). Mathematically, one can write a general first-order parametrization as

$$\overline{w'C'} = -K_C\left(\frac{\partial\overline{C}}{\partial z}\right)+\gamma_C$$

The first term is a local closure, with K_C being the diffusion coefficient, and the scalar C is fluxed down the mean gradient. The second is related to nonlocal effects and is widely used in both the ocean mixed layer and the atmospheric BL.

An example of a nonlocal closure is the mixed layer approach. The approach assumes that potential temperature is constant in height and that the mixed layer is homogeneous in the horizontal. Neglecting horizontal advection, this leads to the simple expression

$\partial\overline{\theta}/\partial t = -(\partial/\partial z)\left(\overline{w'\theta'}\right)$ In the mixed layer approach, $\overline{w'\theta'}$ is assumed to have a constant gradient with height (i.e., the closure utilizes knowledge of gradients spanning the vertical column; it is nonlocal). Also assuming the flux from the surface into the atmosphere or ocean is known—for example, from Monin–Obukhov theory (Foken, 2006)—the only unknown is the flux at the boundary of the mixed layer with the free troposphere or ocean abyss, which is assumed to be due to turbulent entrainment of air or water at the mixed layer interface. The largest source of uncertainty is in specifying this entrainment coefficient. Although this approach was first developed for atmospheric models (Carson, 1973; Lilly, 1968), it was quickly adopted into ocean models (e.g., the Price–Weller–Pinkel scheme; Price et al., 1986), in which it is still widely used due to its computational efficiency (Frants et al., 2013; Lazarevich et al., 2004).

In ocean models, vertical turbulent (diapycnal) mixing acts on all state variables C (temperature, salinity, and momentum). A common approach is the K-profile parametrization (Large et al., 1994), which assumes that the turbulent mixing is dominated by vertical fluxes. It takes the form of a first-order closure with a nonlocal term: $\overline{w'C'} = -\nu_C\left({\partial\overline{C}}/{\partial z}\right)+\nu_C\Gamma_C$, where ν_C is the viscosity/diffusivity associated with C (Large et al., 1994). The diffusivity, ν_C, has several contributions, including resolved and unresolved shear instability, and it depends on both the depth of the BL and a specified vertical shape function that allows for changes in vertical properties within the BL (O'Brien, 1970). The contribution of shear instability is parametrized in terms of the bulk Richardson number, which depends on the buoyancy profile and the horizontal velocity. The depth of the BL is selected as the depth at which the bulk Richardson number equals a set critical value. The nonlocal flux, $\nu_C\Gamma_C$, depends on the prescribed vertical shape function and the surface transport (Van Roekel et al., 2018), which can change based on the process driving the mixing (MacKinnon et al., 2017).

Limitations of Current Parametrizations and Approaches

There are several limitations to the current approach to parametrization development.

Clean Separation of Scales

Current parametrizations have been developed by assuming a clear separation of scales between resolved and unresolved processes (e.g., Arakawa & Schubert, 1974). However, as computing resources, and therefore resolution, increase, many processes become partially resolved. This is often called the *gray zone*. In the gray zone, a process of interest is neither fully resolved nor can it be fully parametrized (e.g., Wyngaard, 2004). This is clearly demonstrated by incrementally coarse-graining large eddy simulation (LES) data and computing both the turbulent fluxes associated with motion smaller than the coarsening scale ("subgrid" motion) and those associated with the "resolved" scales at each resolution (e.g., Dorrestijn et al., 2013). This is shown schematically in figure 6. If one averages over the entire LES domain, naturally all fluxes are unresolved and must be parametrized. Conversely, if one performs no averaging, all fluxes are "resolved." For intermediate length scales, there is a regime in which the unresolved and resolved components of the turbulent flux are of similar magnitudes. This is the gray zone, and the length scales associated with it vary depending on the process of interest (Dorrestijn et al., 2013; Honnert et al., 2020; Pearson et al., 2014). For example, as shown in figure 1, atmospheric organized moist convective systems with length scales of order 10s to 100 km are partially resolved at both typical weather and climate model resolutions (Moncrieff et al., 2017), so traditional parametrization schemes struggle to represent them (Moncrieff, 2019). Scale-aware parametrizations are needed (e.g., Bessac et al., 2021), which can be used in a model across a range of scales, including the gray zone (e.g., Plant & Craig, 2008).

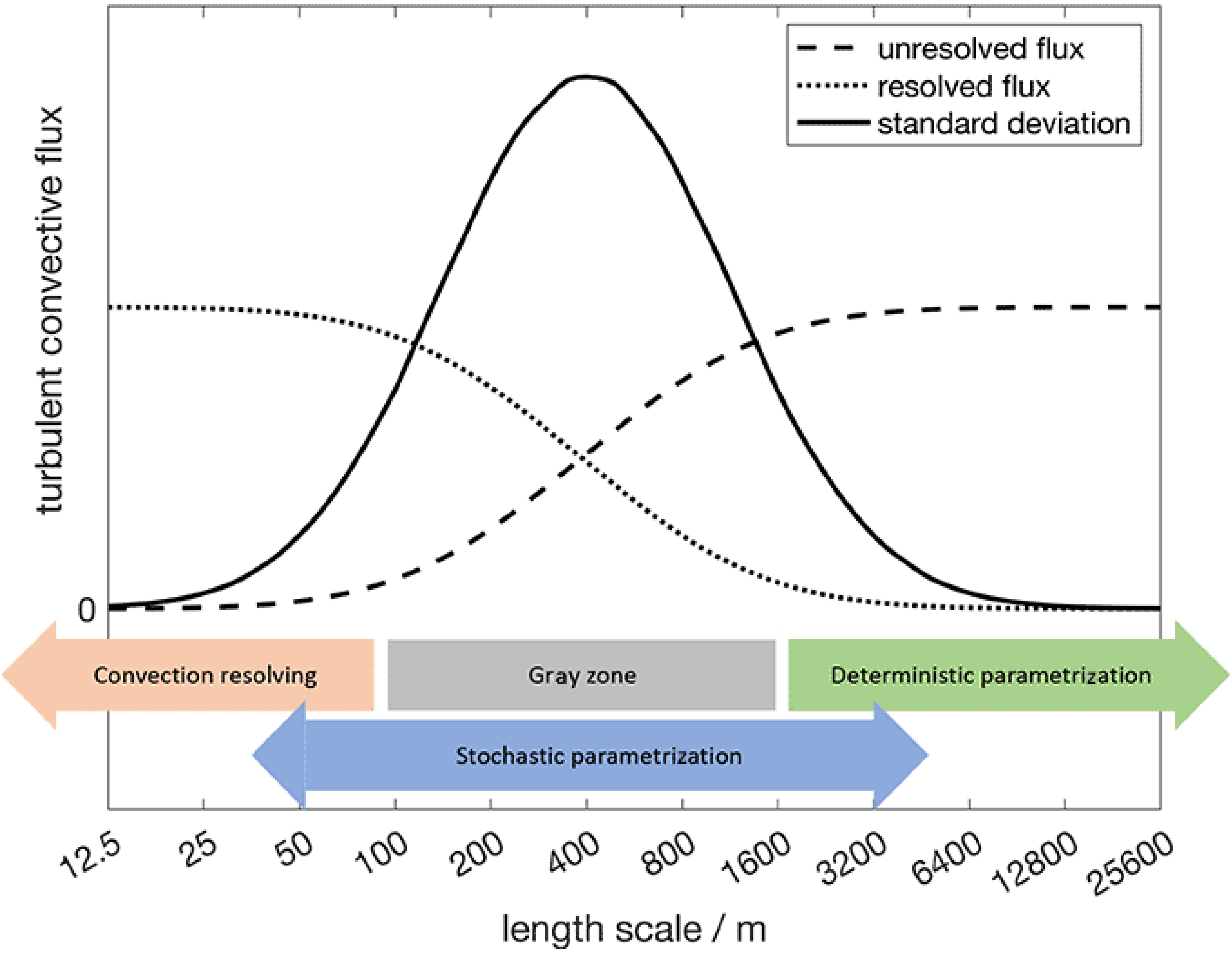

Figure 6. Schematic of resolved and unresolved fluxes associated with a typical small-scale process as a function of grid length scale. In the gray zone, the unresolved and resolved fluxes are both substantial, and there is considerable variability in the unresolved fluxes, necessitating a stochastic approach to parametrization. The length scales on the *x*-axis are typical for the case of atmospheric shallow moist convection.

Source: Adapted from Dorrestijn et al. (2013).

In the ocean, the Rossby deformation radius is the horizontal length scale at which rotation becomes as large as buoyancy. The deformation radius sets the scale of mesoscale eddies, and therefore resolving this scale is critical to capture mesoscale eddies. The current generation of climate models does not resolve this scale in most of the ocean. The deformation length scale associated with the mesoscale eddy gray zone varies with latitude, as shown in figure 7. As the horizontal resolution increases, the mesoscale eddy field becomes partially resolved in some regions of the ocean (Hallberg, 2013). A single parametrization scheme must therefore represent both unresolved and partially resolved eddies. Parametrizations that are flow- and/or resolution-aware have been developed to address these issues (Bachman, 2019; Jansen & Held, 2014; Zanna et al., 2017).

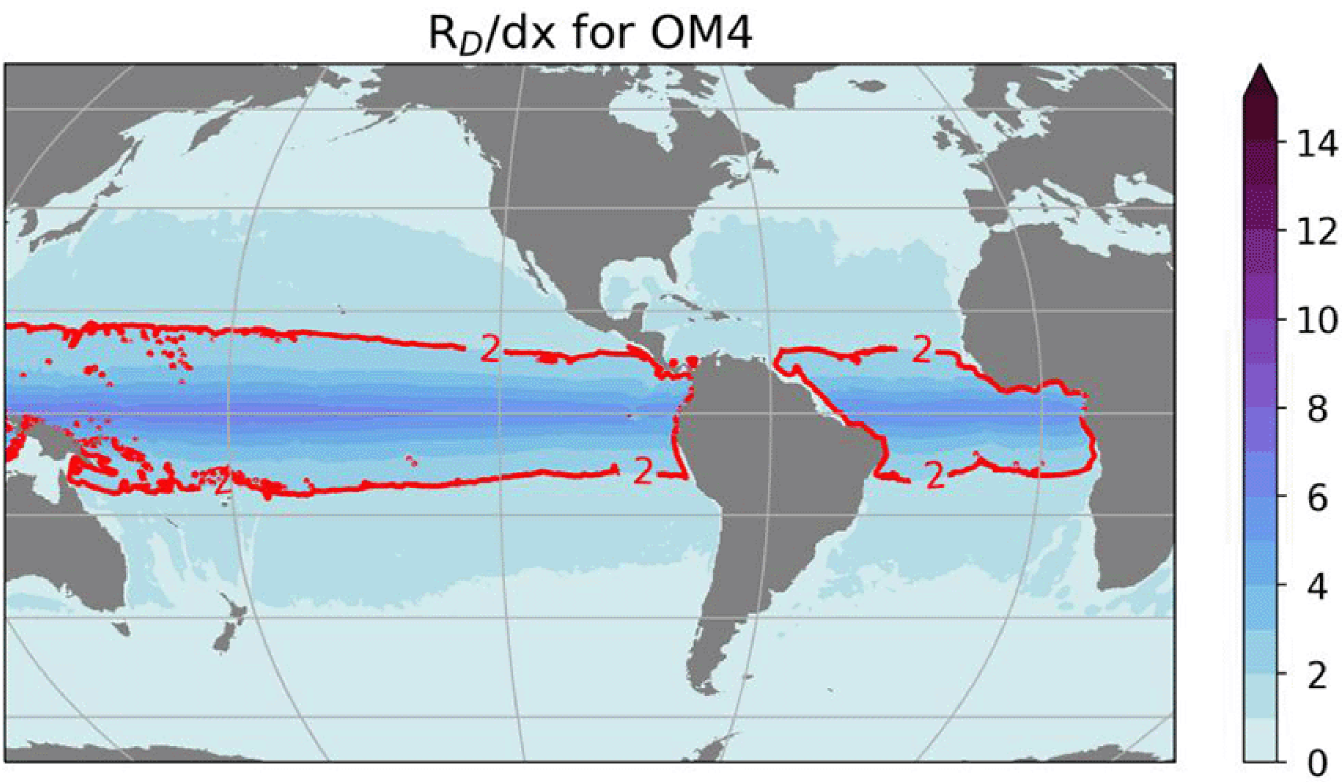

Figure 7. The contours are showing the deformation radius over the model resolution using a global ocean model, GFDL OM4 (Dunne et al., 2020); details of the calculation are given in Hallberg (2013). The tropics are resolving the deformation scale, whereas the mid-latitudes are marginally resolving the deformation scale, defined as the gray zone.

Source: Authors

Separation of Processes

Developing a parametrization scheme generally involves a compartmentalization procedure, whereby related processes within the same medium are dealt with by different parametrization schemes. An example of this in the atmosphere concerns clouds and moist processes. Many global atmospheric models contain separate schemes for BL turbulence, shallow convection, deep convection, and large-scale precipitation (e.g., Gettelman, Mills, et al., 2019; Giorgetta et al., 2018; Hourdin et al., 2020; Walters et al., 2019), whereas in reality, these processes form part of a continuum (Kuang & Bretherton, 2006). Similarly in the ocean, vertical mixing and restratification by the sub-mesoscales are treated separately (Fox-Kemper et al., 2019). This compartmentalization is problematic, particularly with regard to model development. This is because compensating errors between different schemes can mask biases in the model (Palmer & Weisheimer, 2011), such that real improvements to one scheme can lead to degradation to the model simulation.

The Earth system is also split into different components, with separate models to treat processes in the atmosphere, oceans, land surface, etc. These models are often tuned independently before being coupled together (Hourdin et al., 2017; Schmidt et al., 2017). However, biases often develop on coupling, necessitating retuning (Schmidt et al., 2017). Often, biases in one Earth system component can be traced to errors in a different component; for example, persistent biases in the Southern Ocean temperatures can be traced to surface flux biases due to errors in cloud parametrization schemes (Hyder et al., 2018). Accordingly, improving one component can also improve the performance of another component. For example, Kirtman et al. (2012) showed that increasing the resolution of the ocean component of the Community Climate System Model led to improved precipitation patterns. Even the nature of the coupling can affect the model solutions (Rackow & Juricke, 2020). For example, increasing the frequency of the coupling between atmosphere and ocean improves the strength of the Madden–Julian Oscillation in regional (Zhao & Nasuno, 2020) and global (R. Neale, personal communication, 2017) simulations.

Validation and Improvement of Parametrizations

Improvements to parametrization schemes can either be motivated by theoretical arguments (a "bottom up" approach) or designed to correct specific biases in the model (a "top down" approach) (Walters et al., 2019). In both cases, instead of testing parametrization developments in a full climate model, it is common to use single column models (SCMs) to bridge the gap between observations and climate models (Bechtold et al., 2000; Petch et al., 2007; Randall et al., 1996). An SCM consists of a single column taken from a parent global climate model, containing the subgrid parametrization schemes. Boundary forcings are estimated from observations (Zhang et al., 2016) and used in place of the resolved dynamics, before the evolution of the SCM is compared to that observed (Gettelman, Truesdale, et al., 2019). SCMs are computationally cheap to run compared to a global model, enabling sensitivity tests such as vastly enhanced vertical resolution (Hourdin et al., 2019). SCMs can also be compared directly with LESs that resolve small-scale processes of interest (Zhang et al., 2013). However, it can be difficult to interpret SCM results due to the lack of feedback between subgrid processes and the resolved scale dynamics (Dal Gesso & Neggers, 2018).

What Next?

Significant resources are still going into improving the current generation of parametrization schemes. For example, it is possible to refine the selection of mesoscale eddy coefficients in current ocean parametrizations schemes (Hewitt et al., 2020) by invoking conservation of energy in the simulations or tuning them with observations (Couvreux et al., 2021; Hourdin et al., 2021; Schneider, Lan, et al., 2017) or to build on existing approaches to deterministic moist convection parametrization to capture the diurnal cycle better (Bechtold et al., 2014). The further development of process-level understanding, and its incorporation into parametrization schemes, will doubtless continue to improve models. However, there are four new fruitful research directions that each have the potential to give a step-change in model skill.

Unification of Parametrized Processes

As highlighted in the sections on "Atmospheric Parametrizations" and "Limitations of Current Parametrizations and Approaches," traditional approaches to parametrization have addressed groups of processes in separate subroutines. Such compartmentalization is artificial. The early 21st century saw efforts to overcome this limitation in atmospheric models by unifying the parametrization of groups of processes. The unification of moist processes is particularly promising. For example, the eddy-diffusivity mass-flux (EDMF) parametrization (Siebesma et al., 2007; Sušelj et al., 2013, 2014) represents transport within the BLs as arising from two components: An eddy-diffusivity component (see the section on "Turbulent Vertical Mixing in Oceanic and Atmospheric Boundary Layers") represents turbulent transport in neutrally stable regions, and a mass-flux component is used to represent embedded convective motions. Sušelj et al. (2019) extended the approach to include a representation of shallow and deep convection, thereby capturing all moist processes in a single scheme. A key benefit of this unified approach is the lack of trigger functions, which in a modular moist convection parametrization determines whether the scheme is activated or not. Despite aiming to represent the same suite of moist processes, the Cloud Layers Unified By Binormals (CLUBB) approach (Golaz et al., 2002) is very different to EDMF. CLUBB predicts the joint probability distribution function (PDF) of moisture, temperature, and vertical velocity, where the PDF is assumed to be a double Gaussian for computational efficiency. Turbulent fluxes, mass flux, and cloud cover, can be computed from the predicted joint PDF, ensuring consistency between these quantities of interest. Through coupling CLUBB to a microphysics scheme, Storer et al. (2015) extended CLUBB to include a representation of deep convective events. As for EDMF, this formulation avoids the specification of trigger functions for different cloud regimes: The modified scheme is able to capture the smooth transition from stratocumulus cloud regimes to deep convection (Guo et al., 2015).

An alternative approach to unification is *superparametrization*. Here, a two-dimensional cloud resolving model (CRM) of 1- to 4-km resolution is embedded within each grid column of the parent model, replacing the parent model's moist convection and cloud parametrization schemes (Grabowski, 2001; Khairoutdinov & Randall, 2001; Khairoutdinov et al., 2005). The CRM is not re-initialized each timestep and instead runs continuously, introducing memory into the subgrid tendencies. Each CRM is independent of its neighbors, with cyclic boundary conditions, enabling efficient parallelization of the global model. Superparametrization has been shown to improve the diurnal cycle of convective clouds, convective organization and propagation, the representation of the Madden–Julian Oscillation, and the coupling between land and atmosphere (Grabowski, 2001; Kooperman et al., 2016; Pritchard et al., 2011, 2014; Qin et al., 2018). However, the computational cost of the superparametrization approach is substantial compared to conventional parametrization schemes, so it has not been widely adapted. In addition, even a CRM requires parametrization, the details of which can substantially change the behavior of the model solution (Christensen & Driver, 2021).

Unification of mesoscale eddy parameterizations in ocean models has begun. From quasi-geostrophic dynamics, the deformation scale, some of the available potential energy (APE) is transformed into kinetic energy via baroclinic instability and then backscattered to large scales. The transport of tracers in ocean models has been traditionally parametrized via the Gent–McWilliams (GM) framework, which mimics baroclinic instability. The framework leads to a flattening of isopycnals and net sink of APE. This net loss of APE is unaccounted for in the traditional GM framework. Early 21st-century advances in mesoscale eddy parametrizations have focused on closing the mesoscale eddy energy budget (Cessi, 2008; Marshall & Adcroft, 2010; Marshall et al., 2012). In particular, new parametrizations of eddy momentum have been devised to address the kinetic energy backscatter (from small to large scales) (Jansen & Held, 2014; Juricke et al., 2017; Porta Mana & Zanna, 2014; Zanna et al., 2017) and to address the transformation of lost APE into kinetic energy (Bachman, 2019; Jansen & Held, 2014; Zanna & Bolton, 2020). This unification of mesoscale eddy parametrizations is done primarily by focusing on the mesoscale eddy energy budget, but it is not yet operational.

Stochastic Parametrization

Another fruitful approach since the late 1990s has been the development of stochastic parametrizations. Here, the parametrization scheme is formulated in terms of a PDF constrained by the resolved scale flow. This encapsulates the statistical nature of many subgrid processes in the absence of scale separation, and it is particularly appropriate at gray zone resolutions, where there is high variability (i.e., uncertainty) in the subgrid motions consistent with the resolved scales (see figure 6).

Stochastic parametrizations have several advantages over deterministic parametrizations. A stochastic framework is more consistent with the underlying Navier–Stokes equations, which show strong evidence of scaling symmetries (Lovejoy & Schertzer, 2013; Nastrom & Gage, 1985). Stochastic parametrizations can be derived on theoretical grounds—for example, homogenization theory, which decomposes the fast and slow scales of interest—or by using statistical mechanics (e.g., Craig & Cohen, 2006) for the parametrizations of subgrid convective cloud mass flux. Alternatively, stochastic parametrizations can be guided by data—for example, by coarse-graining the output of a high-resolution simulation to diagnose missing or uncertain processes in a coarse-resolution model (for atmospheric convection, see Shutts & Palmer, 2007; see also the Appendix). Figure 8 shows the results of one such coarse-graining study (Christensen, 2020). The "true" subgrid tendency is diagnosed from a coarse-grained high-resolution data set and compared to the tendency predicted by a low-resolution model initialized from the same coarse-grained fields. Although the parametrized tendency is a good predictor of the mean of the "true" tendency, as expected, substantial variability is observed about this mean. This variability increases as the parametrized mean increases, motivating a state-dependent or multiplicative stochastic correction term (Buizza et al., 1999). This provides further evidence that parametrization schemes should be stochastic and can also be used to motivate the form that stochastic parametrizations should take (Christensen, 2020; Porta Mana & Zanna, 2014).

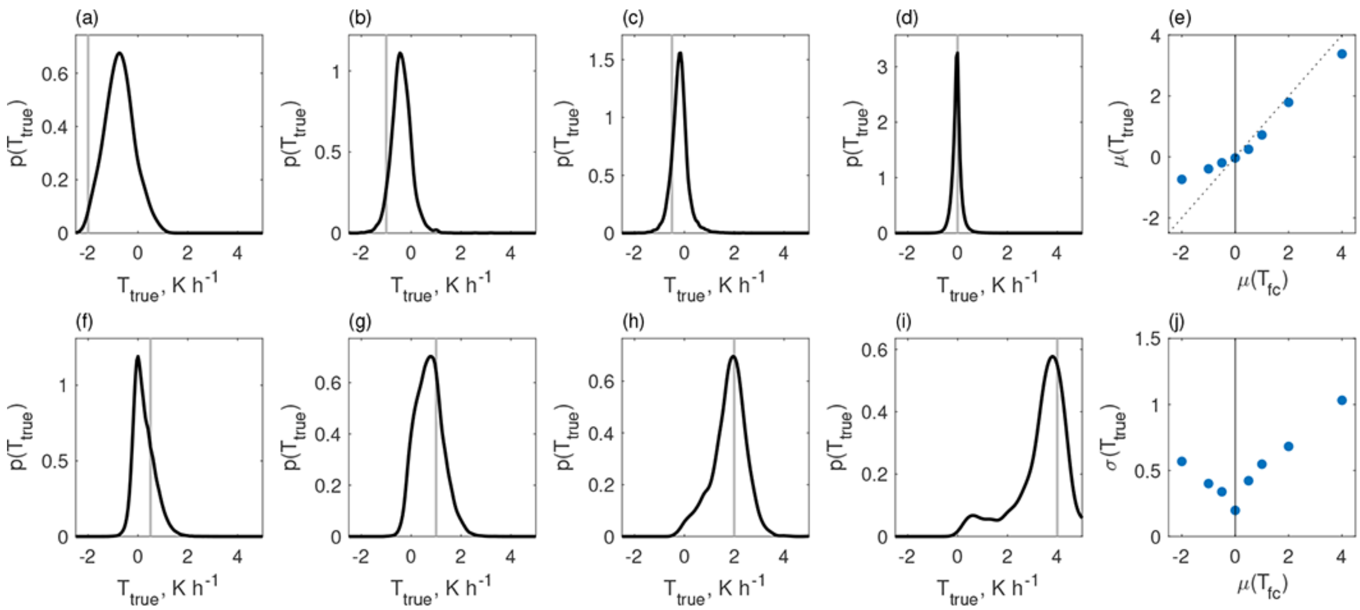

Figure 8. (a–d, f–i) Probability distribution functions of "true" diagnosed tendency for temperature at 850 hPa computed from a high-resolution simulation, conditioned on the tendency predicted by a low-resolution forecast model. The narrow gray rectangle in each panel indicates the forecast tendency. (e) Mean "true" tendency conditioned on predicted tendency. For this model, negative temperature tendencies are cold biased. (j) Standard deviation of "true" tendency conditioned on predicted tendency. Uncertainty in the "true" tendency increases with the magnitude of the forecast tendency.

Source: Adapted from Christensen (2020).

From a practical standpoint, stochastic parametrizations can also represent uncertainty associated with the parametrization itself. It is necessary to represent this *model uncertainty* to produce reliable ensemble forecasts on weather, subseasonal and seasonal timescales (Berner et al., 2017). For this reason, stochastic parametrizations are widely used across these communities. The climate modeling community has also begun to experiment with using stochastic parametrizations. Including stochasticity in climate models can improve systematic biases, including those in the mean state, such as the distribution of precipitation (Strommen et al., 2019) and biases in modes of variability (Juricke et al., 2017), such as the El Nino–Southern Oscillation (Christensen et al., 2017).

Machine Learning Parametrizations

Since the early 21st century, the advent and efficiency of machine learning (ML) algorithms have allowed for more accurate data-driven parametrizations. In this case, by using data from high-resolution simulations and/or observations, the ML algorithm is tasked to obtain an optimal relationship between the subgrid forcing and the resolved variables (figure 9), where the subgrid and resolved scales are separated using a coarse-graining approach (see the Appendix). A host of ML methods are available. However, deep learning has been shown to be well-suited to extract subgrid parametrizations using spatiotemporal information. For example, neural networks have been shown to be a useful tool for turbulence parametrization in idealized setups (Ling et al., 2016; Maulik & San, 2017; Maulik et al., 2019). In more complex settings, neural network-based convective cloud parametrizations have been shown to outperform traditional physics-driven parametrizations when implemented in coarse resolution weather and climate models (Brenowitz & Bretherton, 2018; Gentine et al., 2018; Yuval et al., 2021). In the ocean, convolutional neural networks have been successfully used to parametrize ocean mesoscale eddies (Bolton & Zanna, 2019; Zanna & Bolton, 2020) and vertical mixing (Salehipour & Peltier, 2019) efficiently. New ML methods are also being tested in the simple chaotic Lorenz model—generative adversarial networks for stochastic subgrid parametrizations (Gagne et al. 2020) and transfer learning to best optimize ML parametrizations (Subel et al., 2021) are notable examples.

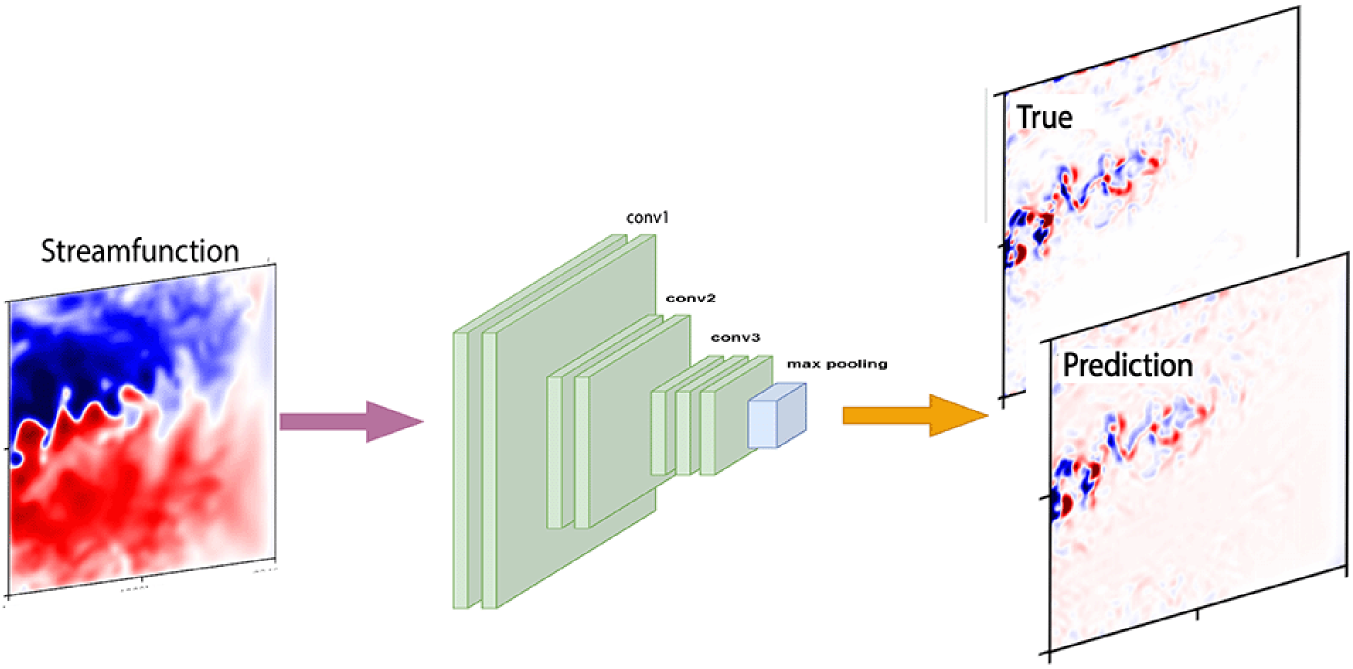

Figure 9. Parametrization with machine learning, based on Bolton and Zanna (2019): streamfunction as input to a convolutional neural network to predict the zonal component of the sub-grid forcing, S_x.

Source: Authors

Instead of learning improved parametrizations, ML can also be used as a tool to speed up existing schemes. Studies in the late 20th century successfully emulated radiation schemes (Chevallier et al., 1998; Krasnopolsky et al., 2005), which are notoriously expensive. Substantial breakthroughs in deep learning in the early 2010s paved the way for work that revisited radiation (Veerman et al., 2021) and have targeted emulation of other schemes, including moist convection (O'Gorman & Dwyer, 2018) and gravity wave drag (Chantry et al., 2021). Although ML can often be seen as a black box, emerging ideas to improve ML methods are being proposed. Tools can be used to interpret results, from heat maps (Ham et al., 2019) to learning differential equations (Zanna &

Bolton, 2020): These tools are a way forward to open the black box of ML parametrizations. Yet many challenges remain; see the section on "Challenges and Opportunities" for further discussion.

Novel Validation Approaches

New approaches in parametrization need novel validation approaches. Although the basic questions of physical consistency and impact on model biases must always be evaluated, probabilistic parametrizations have additional degrees of freedom that are more difficult to assess. One approach is the use of data assimilation to attribute errors in the forecast to the deficiency in physics, observational errors, and model biases (Klinker & Sardeshmukh, 1992; Rodwell & Palmer, 2007; Rodwell et al., 2016). A key benefit of studying analysis increments is that verification occurs on a sufficiently short timescale as to be uncontaminated by errors from remote parts of the world. The key limitation is that it cannot assess errors that grow on longer timescales (e.g., due to coupled processes) (Christensen & Berner, 2019). Developments in ensemble data assimilation allow partitioning of error covariance into observational uncertainty, bias, and ensemble variance to check for consistency in a probabilistic framework (Rodwell et al., 2016, 2018). This closely assesses the performance of stochastic parametrizations.

An alternative is the use of reanalysis data sets to initialize short (3–5 days) climate model simulations (e.g., Hannay et al., 2009; Medeiros et al., 2012; Williams et al., 2013). Verification is possible for these short-range forecasts, which can be directly compared to observations. The short duration allows for some localization of errors, allowing errors to be attributed to a particular parametrization scheme, thereby targeting analysis of fast physics biases (Williams et al., 2013). For example, tests with the CMIP6 version of the Met Office model show improved initial tendencies compared to earlier model versions, providing reassurance about the fidelity of fast cloud processes in the model, in the face of an elevated climate sensitivity (Williams et al., 2020).

These novel approaches to validation suggest that a seamless approach to modeling the Earth system across a range of timescales should be taken (Bauer et al., 2015; Brunet et al., 2010; Hurrell et al., 2009; Phillips et al., 2004). This involves the weather, seasonal and climate communities working together to produce and evaluate models. The fast processes in a climate model can be tested by using that model for initialized forecasts, where verification is possible (Palmer et al., 2008; Weisheimer & Palmer, 2014), before being used for long-range projections.

Challenges and Opportunities

This section highlights outstanding problems to be solved in parametrization, many of which are common across traditional and novel approaches.

Interaction

It is not necessarily practical to develop a single parametrization scheme for all subgrid processes in the atmosphere or ocean. Resources must be invested to improve the coupling between individual schemes and to identify and reduce compensating biases. Lessons can be learned from the experience of coupling separate Earth system components, including the benefits and limitations of testing subroutines individually and the importance of the nature of the coupling (Ginu-Bogdan et al., 2018). In contrast to traditional parametrization, early approaches to stochastic or machine-learned parametrization have been holistic and use a single stochastic approach (Buizza et al., 1999) or neural network to represent all subgrid processes (e.g., Yuval et al., 2021). Here, there is increasing interest in moving to a targeted approach whereby a bespoke scheme is developed for each process of interest (Ollinaho et al., 2017). It is not clear how many such schemes can be constrained or how they would subsequently interact with each other, but lessons can be learned from past experience with traditional schemes.

Scale Awareness

Parametrization schemes must perform well across a wide range of resolutions. Atmospheric schemes are employed across weather, seasonal and climate models, whereas ocean parametrization schemes may experience different resolutions even within the same simulation (Wang et al., 2014). For ocean parametrizations, the problem is compounded by the varying Rossby radius of deformation, which sets the scale of ocean eddies (see figure 7). Research into scale-aware parametrizations could include physical understanding of the nature of processes across scales or data-driven approaches (Bessac et al., 2021).

Universality

Developing a new parametrization scheme involves a substantial investment of resources, both human and computational. To what extent can a parametrization scheme (traditional, stochastic, or machine-learned) developed for one model be transferred to another model? Critical for climate prediction, how universal or generalizable are our parametrizations? It is assumed that traditional schemes based on the laws of physics are appropriate in different climates, although it is not known whether the characteristics of errors in those schemes may change. The extent to which a data-driven parametrization generalizes to a different climate state is an open question requiring further research.

Conservation

The laws of physics dictate that energy, mass, and momentum be conserved. Yet many parametrization schemes do not obey these conservation laws such that conservation “fixers” are routinely employed in numerical models (e.g., Williamson et al., 2015). It has been difficult to impose conservation laws in some stochastic schemes without changing other assumptions in the schemes (Davini et al., 2017; Sanchez et al., 2016). In machine learning (ML) parametrizations, conservation laws and symmetry can be imposed either as part of the algorithm or in the loss function: This type of physics-constrained ML parametrization has the advantage of respecting the underlying physics (Beucler et al., 2021).

Stability

Stability of forecasts has been a problem since Richardson's first numerical weather prediction (Lynch, 2006). Many models use implicit and/or semi-Lagrangian approaches to improve stability and allow longer timesteps (e.g., Cullen, 2001). However, numerical stability continues to impose constraints when developing parametrizations (e.g., Beljaars et al., 2017; Leutbecher et al., 2017). ML parametrizations in particular suffer from this problem: Parametrizations that perform well during training can prove unstable when run in "online" mode, with substantial work ongoing to understand and resolve this problem (e.g., Brenowitz & Bretherton, 2018; Yuval & O'Gorman, 2020; Yuval et al., 2021).

Data

Stochastic and ML approaches to parametrization are both data-driven. They rely on the availability of high-resolution data, spanning large areas and for extended periods of time. The lack of suitable observational data has led to a reliance on model data. However, such model simulations still require subgrid parametrizations and contain their own biases. Furthermore, simulations are expensive to produce, limiting the size of the training data set and the potential universality of the resultant scheme. Although they are not built based on data, traditional parametrizations also suffer from a lack of observational data. Stringent tests on parametrization schemes require high-quality observational data. For atmospheric schemes, this takes the form of data from an array of observational platforms, including balloon soundings and surface instruments (Zhang et al., 2016). There are only a few sites globally with this capability, giving rise to representativity issues. In the ocean, although satellite altimetry and global float programs such as Argo have revolutionized our understanding of the ocean, these data sets by themselves are not sufficiently high resolution to devise data-driven parametrization but may complement model data.

Acknowledgment

H. C. was funded by Natural Environment Research Council grant NE/P018238/1. L. Z. was supported in part by grants NSFGEO 1912357 and NOAA CVP NA19OAR4310364. This research is supported in part by the generosity of Eric and Wendy Schmidt by recommendation of Schmidt Futures, as part of its Virtual Earth System Research Institute (VESRI). The authors are grateful to Elizabeth Yankovsky for creating figure 7.

Further Reading

Textbooks

Griffies, S. (2004). *Fundamentals of ocean climate models*. Princeton University Press.

Stensrud, D. J. (2007). *Parameterization schemes: Keys to understanding numerical weather prediction models*. Cambridge University Press.

Tomkins Warner, T. (2011). *Numerical weather and climate prediction models*. Cambridge University Press.

Classic Papers

Arakawa, A., & Schubert, W. H. (1974). Interaction of a cumulus cloud ensemble with the large-scale environment, Part I. *Journal of the Atmospheric Sciences*, *31*, 674–701.

Gent, P. R., & McWilliams, J. C. (1990). Isopycnal mixing in ocean circulation models. *Journal of Physical Oceanography*, *20*(1), 150–155.

Manabe, S., & Wetherald, R. T. (1967). Thermal equilibrium of the atmosphere with a given distribution of relative humidity. *Journal of the Atmospheric Sciences*, *24*(3), 241–259.

Model Description

Because such papers are typically more transient, the authors recommend seeking out internal documentation, such as those published for each operational cycle of the European Centre for Medium-Range Weather Forecasts <https://www.ecmwf.int/en/publications/ifs-documentation>' Integrated Forecasting System.

State of the Art

Berner, J., Achatz, U., Batt, L., Bengtsson, L., de la Camara, A., Christensen, H. M., Colangeli, M., Coleman, D. R. B., Crommelin, D., Dolaptchiev, S. I., Franzke, L. E., Friederichs, P., Imkeller, P., Jarvinen, H., Juricke, S., Kitsios, V., Lott, F., Lucarini, V., Mahajan, S., . . . Yano, J.-I. (2017). Stochastic parameterization toward a new view of weather and climate models. *Bulletin of the American Meteorological Society*, *98*(3), 565–588.

Bolton, T., & Zanna, L. (2019). Applications of deep learning to ocean data inference and subgrid parameterization. *Journal of Advances in Modeling Earth Systems*, *11*(1), 376–399.

Buizza, R., Miller, M., & Palmer, T. N. (1999). Stochastic representation of model uncertainties in the ECMWF ensemble prediction system <https://doi.org/10.1256/smsqj.56005>. *Quarterly Journal of the Royal Meteorological Society*, *125*(560), 2887–2908.

Camps-Valls, G., Tuia, D., Zhu, X. X., & Reichstein, M. (2021). *Deep learning for the Earth sciences: A comprehensive approach to remote sensing, climate science, and geosciences* (Chapters 20 and 21). Wiley.

Gentine, P., Pritchard, M., Rasp, S., Reinaudi, G., & Yacalis, G. (2018). Could machine learning break the convection parameterization deadlock? *Geophysical Research Letters*, *45*(11), 5742–5751.

Golaz, J.-C., Larson, V. E., & Cotton, W. R. (2002). A PDF-based model for boundary layer clouds: Part I: Method and model description <*https://doi.org/10.1175/1520-0469(2002)059%3c3540:APBMFB%3e2.0.CO;2*>. *Journal of the Atmospheric Sciences*, *59*(24), 3540–3551.

Hewitt, H. T., Roberts, M., Mathiot, P., Biastoch, A., Blockley, E., Chassignet, E. P., & Zhang, Q. (2020). Resolving and parameterising the ocean mesoscale in Earth system models. *Current Climate Change Reports*, *6*(4), 137–152.

References

Abdalla, S., Isaksen, L., Janssen, P., & Wedi, N. (2013). Effective spectral resolution of ECMWF atmospheric forecast models <*https://doi.org/10.21957/rue4o7ac*>. *ECMWF Newsletter*, *137*, 19–22.

Arakawa, A., & Schubert, W. H. (1974). Interaction of a cumulus cloud ensemble with the large-scale environment, Part I. *Journal of the Atmospheric Sciences*, *31*, 674–701.

Bachman, S. D. (2019). The GM + E closure: A framework for coupling backscatter with the Gent and McWilliams parameterization. *Ocean Modelling*, *136*, 85–106.

Bachman, S. D., Fox-Kemper, B., & Pearson, B. (2017). A scale-aware subgrid model for quasi-geostrophic turbulence. *Journal of Geophysical Research: Oceans*, *122*(2), 1529–1554.

Balaji, V. (2021). Climbing down Charney's ladder: Machine learning and the post-Dennard era of computational climate science <*https://doi.org/10.1098/rsta.2020.0085*>. *Philosophical Transactions of the Royal Society A*, *379*(2194).

Bassil, N. (2014). Accuracy of early GFS and ECMWF Sandy (2012) track forecasts: Evidence for dependence on cumulus parameterization <*https://doi.org/10.1002/2014GL059839*>. *Geophysical Research Letters*, *41*(9), 3274–3281.

Bauer, P., Stevens, B., & Hazeleger, W. (2021). A digital twin of Earth for the green transition <*https://doi.org/10.1038/s41558-021-00986-y*>. *Nature Climate Change*, *11*(2), 80–83.

Bauer, P., Thorpe, A., & Brunet, G. (2015). The quiet revolution of numerical weather prediction <*https://doi.org/10.1038/nature14956*>. *Nature*, *525*(7567), 47–55.

Bechtold, P., Bazile, E., Guichard, F., Mascart, P., & Richard, E. (2001). A mass-flux convection scheme for regional and global models <*https://rmets.onlinelibrary.wiley.com/doi/10.1002/qj.49712757309*>. *Quarterly Journal of the Royal Meteorological Society*, *127*(573), 869–886.

Bechtold, P., Redelsperger, J.-L., Beau, I., Blackburn, M., Brinkop, S., Grandpeix, J.-Y., Grant, A., Gregory, D., Guichard, F., Hoff, C., & Ionnidou, E. (2000). A GCSS model intercomparison for a tropical squall line observed during TOGA-COARE. 11: Intercomparison of single-column models and a cloud-resolving model. *Quarterly Journal of the Royal Meteorological Society*, *126*(564), 865–888.

Bechtold, P., Semane, N., Lopez, P., Chaboureau, J.-P., Beljaars, A., & Bormann, N. (2014). Representing equilibrium and nonequilibrium convection in large-scale models <*https://doi.org/10.1175/JAS-D-13-0163.1*>. *Journal of the Atmospheric Sciences*, *71*(2), 734–753.

Beljaars, A., Dutra, E., Balsamo, G., & Lemarié, F. (2017). On the numerical stability of surface–atmosphere coupling in weather and climate models <https://doi.org/10.5194/gmd-10-977-2017>. *Geoscientific Model Development*, *10*(2), 977–989.

Berner, J., Achatz, U., Batte, L., de la Camara, A., Christensen, H., Colangeli, M., Coleman, D. R., Crommelin, D., Dolaptchiev, S., Franzke, L. E., Friederichs, P., Imkeller, P., Järvinen, H., Juricke, S., Kitsios, V., Lott, F., Lucarini, V., Mahajan, S., Palmer, T. N., . . . Yano, Y.-I. (2017). Stochastic parameterization: Towards a new view of weather and climate models. *Bulletin of the American Meteorological Society*, *98*, 565–588.

Bessac, J., Christensen, H. M., Endo, K., Monahan, A. H., & Weitzel, N. (2021). Scale-aware space–time stochastic parameterization of subgrid-scale velocity enhancement of sea surface fluxes <https://doi.org/10.1029/2020MS002367>. *Journal of Advances in Modeling Earth Systems*, *13*(4), 1–23.

Betts, A. K. (1986). A new convective adjustment scheme. Part I: Observational and theoretical basis. *Quarterly Journal of the Royal Meteorological Society*, *112*, 677–691.

Beucler, T., Pritchard, M., Rasp, S., Ott, J., Baldi, P., & Gentine, P. (2021). Enforcing analytic constraints in neural networks emulating physical systems. *Physical Review Letters*, *9*(126), 098302.

Bogenschutz, P. A., Gettelman, A., Morrison, H., Larson, V. E., Craig, C., & Schanen, D. P. (2013). Higher-order turbulence closure and its impact on climate simulations in the community atmosphere model <https://doi.org/10.1175/JCLI-D-13-00075.1>. *Journal of Climate*, *26*(23), 9655–9676.

Bolton, T., & Zanna, L. (2019). Applications of deep learning to ocean data inference and subgrid parameterization <https://doi.org/10.1029/2018MS001472>. *Journal of Advances in Modeling Earth Systems*, *11*(1), 376–399.

Brenowitz, N. D., & Bretherton, C. S. (2018). Prognostic validation of a neural network unified physics parameterization <https://doi.org/10.1029/2018GL078510>. *Geophysical Research Letters*, *45*, 6289–6298.

Brunet, G., Shapiro, M., Hoskins, B., Moncrieff, M., Dole, R., Kiladis, G. N., Kirtman, B., Lorenc, A., Mills, B., Morss, R., Polavarapu, S., Rogers, D., Schaake, J., & Shukla, J. (2010). Collaboration of the weather and climate communities to advance subseasonal-to-seasonal prediction <https://doi.org/10.1175/2010BAMS3013.1>. *Bulletin of the American Meteorological Society*, *91*(10), 1397–1406.

Bryan, G. H., Wyngaard, J. C., & Michael Fritsch, J. (2003). Resolution requirements for the simulation of deep moist convection <https://doi.org/10.1175/1520-0493(2003)131%3c2394:RRFTSO%3e2.0.CO;2>. *Monthly Weather Review*, *131*(10), 2394–2416.

Buizza, R., Miller, M., & Palmer, T. N. (1999). Stochastic representation of model uncertainties in the ECMWF ensemble prediction system <https://doi.org/10.1256/smsqj.56005>. *Quarterly Journal of the Royal Meteorological Society*, *125*(560), 2887–2908.

Cagnazzo, C., Manzini, E., Giorgetta, M. A., Forster, P. M. D. F., & Morcrette, J. J. (2007). Impact of an improved shortwave radiation scheme in the MAECHAM5 general circulation model <https://doi.org/10.5194/acp-7-2503-2007>. *Atmospheric Chemistry and Physics*, *7*(10), 2503–2515.

Caldwell, P. M., Mametjanov, A., Tang, Q., Van, L. P., Golaz, J.-C., Lin, W., Bader, D. C., Keen, N. D., Feng, Y., Jacob, R., Maltrud, M. E., Roberts, A. F., Taylor, M. A., Veneziani, M., Wang, H., Wolfe, J. D., Balaguru, K., Cameron-Smith, P., Dong, L., . . . Zhou, T. (2019). The DOE E3SM coupled model Version 1: Description and results at high resolution. *Journal of Advances in Modeling Earth Systems*, *11*(12), 4095–4146.

Carson, D. J. (1973). The development of a dry inversion-capped convectively unstable boundary layer <https://doi.org/10.1002/qj.49709942105>. *Quarterly Journal of the Royal Meteorological Society*, *99*(421), 450–467.

Carton, J. A., Grodsky, S. A., & Liu, H. (2008). Variability of the oceanic mixed layer, 1960–2004 <https://doi.org/10.1175/2007JCLI1798.1>. *Journal of Climate*, *21*(5), 1029–1047.

Cessi, P. (2008). An energy-constrained parameterization of eddy buoyancy flux. *Journal of Physical Oceanography*, *38*(8), 1807–1819.

Chantry, M., Hatfield, S., Duben, P., Polichtchouk, I., & Palmer, T. (2021). Machine learning emulation of gravity wave drag in numerical weather forecasting <http://arxiv.org/abs/2101.08195>. *Journal of Advances in Modeling Earth Systems*, *13*(7), e2021MS002477.

Chevallier, F., Cheruy, F., Scott, N. A., & Chedin, A. (1998). A neural network approach for a fast and accurate computation of a longwave radiative budget <https://journals.ametsoc.org/view/journals/apme/37/11/1520-0450_1998_037_1385_annafa_2.0.co_2.xml>. *Journal of Applied Meteorology*, *37*(11), 1385–1397.

Christensen, H. M. (2020). Constraining stochastic parametrisation schemes using high-resolution simulations. *Quarterly Journal of the Royal Meteorological Society*, *146*(727), 938–962.

Christensen, H. M., & Berner, J. (2019). From reliable weather forecasts to skilful climate response: A dynamical systems approach. *Quarterly Journal of the Royal Meteorological Society*, *145*(720), 1052–1069.

Christensen, H. M., Berner, J., Coleman, D. R. B., & Palmer, T. N. (2017). Stochastic parameterization and El Niño-southern oscillation <https://journals.ametsoc.org/view/journals/clim/30/1/jcli-d-16-0122.1.xml>. *Journal of Climate*, *30*(1), 17–38.

Christensen, H. M., & Driver, O. (2021). The fractal nature of clouds in global storm-resolving models. *Geophysical Research Letters*, *48*(23), e2021GL095746.

Couvreux, F., Hourdin, F., Williamson, D., Roehrig, R., Volodina, V., Villefranque, N., Rio, C., Audouin, O., Salter, J., Bazile, E., Brient, F., Favot, F., Honnert, R., Lefebvre, M. P., Madeleine, J. B., Rodier, Q., & Xu, W. (2021). Process-based climate model development harnessing machine learning: I. A calibration tool for parameterization improvement <https://doi.org/10.1029/2020MS002217>. *Journal of Advances in Modeling Earth Systems*, *13*(3), 1–27.

Craig, G. C., & Cohen, B. G. (2006). Fluctuations in an equilibrium convective ensemble. Part I: Theoretical formulation <https://doi.org/10.1175/JAS3709.1>. *Journal of the Atmospheric Sciences*, *63*(8), 1996–2004.

Cronin, M. F., Gentemann, C. L., Edson, J., Ueki, I., Bourassa, M., Brown, S., Clayson, C. A., Fairall, C. W., Farrar, J. T., Gille, S. T., Gulev, S., Josey, S. A., Kato, S., Katsumata, M., Kent, E., Krug, M., Minnett, P. J., Parfitt, R., Pinker, R. T., ... Zhang, D. (2019). Air–sea fluxes with a focus on heat and momentum <https://www.frontiersin.org/articles/10.3389/fmars.2019.00430/full>. *Frontiers in Marine Science*, *6*, 430.

Cullen, M. P. J. (2001). Alternative implementations of the semi-Lagrangian semi-implicit schemes in the ECMWF model. *Quarterly Journal of the Royal Meteorological Society*, *127*, 2787–2802.

Dal Gesso, S., & Neggers, R. A. J. (2018). Can we use single-column models for understanding the boundary layer cloud–climate feedback? <https://doi.org/10.1002/2017MS001113> *Journal of Advances in Modeling Earth Systems*, *10*(2), 245–261.

Davini, P., von Hardenberg, J., Corti, S., Christensen, H. M., Juricke, S., Subramanian, A., Watson, P. A. G., Weisheimer, A., & Palmer, T. N. (2017). Climate sphinx: Evaluating the impact of resolution and stochastic physics parameterisations in the EC-Earth global climate model. *Geoscientific Model Development*, *10*(3), 1383–1402.

Davy, R. (2018). The climatology of the atmospheric boundary layer in contemporary global climate models <https://doi.org/10.1175/JCLI-D-17-0498.1>. *Journal of Climate*, *31*(22), 9151–9173.

Davy, R., & Esau, I. (2014). Global climate models' bias in surface temperature trends and variability <https://doi.org/10.1088/1748-9326/9/11/114024>. *Environmental Research Letters*, *9*(11), 114024.

Davy, R., & Esau, I. (2016). Differences in the efficacy of climate forcings explained by variations in atmospheric boundary layer depth <https://doi.org/10.1038/ncomms11690>. *Nature Communications*, *7*, 1–8.

Degrazia, G. A., Anfossi, D., Carvalho, J. C., Mangia, C., Tirabassi, T., & Campos Velho, H. F. (2000). Turbulence parameterisation for PBL dispersion models in all stability conditions <https://doi.org/10.1016/S1352-2310(00)00116-3>. *Atmospheric Environment*, *34*(21), 3575–3583.

Dickey, T. D. (2001). The role of new technology in advancing ocean biogeochemical research <https://doi.org/10.5670/oceanog.2001.11>. *Oceanography*, *14*(4), 108–120.

Donner, L. J., Seman, C. J., Hemler, R. S., & Fan, S. (2001). A cumulus parameterization including mass fluxes, convective vertical velocities, and mesoscale effects: Thermodynamic and hydrological aspects in a general circulation model <https://journals.ametsoc.org/view/journals/clim/14/16/1520-0442_2001_014_3444_acpimf_2.0.co_2.xml>. *Journal of Climate*, *14*(16), 3444–3463.

Dorrestijn, J., Crommelin, D. T., Siebesma, A. P., & Jonker, H. J. J. (2013). Stochastic parameterization of shallow cumulus convection estimated from high-resolution model data. *Theoretical and Computational Fluid Dynamics*, *27*(1–2), 133–148.

Döscher, R., Acosta, M., Alessandri, A., Anthoni, P., Arneth, A., Arsouze, T., Bergmann, T., Bernadello, R., Bousetta, S., Caron, L.-P., Carver, G., Castrillo, M., Catalano, F., Cvijanovic, I., Davini, P., Dekker, E., Doblas-Reyes, F. J., Docquier, D., Echevarria, P., . . . Zhang, Q. (2021). The EC-Earth3 Earth system model for the climate model intercomparison project 6 <https://doi.org/10.5194/gmd-2020-446>. *Geoscientific Model Development Discussions*, *2021*, 1–90.

Dunne, J. P., Horowitz, L. W., Adcroft, A. J., Ginoux, P., Held, I. M., John, J. G., Krasting, J. P., Malyshev, S., Naik, V., Paulot, F., Shevliakova, E., Stock, C. A., Zadeh, N., Balaji, V., Blanton, C., Dunne, K. A., Dupuis, C., Durachta, J., Dussin, R., . . . Zhao, M. (2020). The GFDL Earth System Model Version 4.1 (GFDL-ESM 4.1): Overall coupled model description and simulation characteristics <https://doi.org/10.1029/2019MS002015>. *Journal of Advances in Modeling Earth Systems*, *12*(11), e2019MS002015.

Etling, D., & Brown, R. A. (1993). Roll vortices in the planetary boundary layer: A review <https://doi.org/10.1007/BF00705527>. *Boundary-Layer Meteorology*, *65*(3), 215–248.

Foken, T. (2006). 50 years of the Monin–Obukhov similarity theory <https://doi.org/10.1007/s10546-006-9048-6>. *Boundary-Layer Meteorology*, *119*(3), 431–447.

Fox-Kemper, B., Adcroft, A., Böning, C. W., Chassignet, E. P., Curchitser, E., Danabasoglu, G., Eden, C., England, M. H., Gerdes, R., Greatbatch, R. J., Griffies, S. M., Hallberg, R. W., Hanert, E., Heimbach, P., Hewitt, H. T., Hill, C. N., Komuro, Y., Legg, S., Le Sommer, J., . . . Yeager, S. G. (2019). Challenges and prospects in ocean circulation models. *Frontiers in Marine Science*, *6*, Article 65.

Fox-Kemper, B., Ferrari, R., & Hallberg, R. (2008). Parameterization of mixed layer eddies. Part I: Theory and diagnosis. *Journal of Physical Oceanography*, *38*(6), 1145–1165.

Frants, M., Gille, S. T., Hatta, M., Hiscock, W. T., Kahru, M., Measures, C. I., Mitchell, B. G., & Zhou, M. (2013). Analysis of horizontal and vertical processes contributing to natural iron supply in the mixed layer in southern Drake Passage <https://doi.org/10.1016/j.dsr2.2012.06.001>. *Deep-Sea Research Part II*, *90*, 68–76.

Gagne, D. J., II, Christensen, H. M., Subramanian, A. C., & Monahan, A. H. (2020). Machine learning for stochastic parameterization: Generative adversarial networks in the Lorenz ’96 model <https://agupubs.onlinelibrary.wiley.com/doi/full/10.1029/2019MS001896>. *Journal of Advances in Modeling Earth Systems*, *12*(3), e2019MS001896.

Garratt, J. R. (1993). Sensitivity of climate simulations to land-surface and atmospheric boundary-layer treatments—A review. *Journal of Climate*, *6*, 419–448.

Gent, P. R., & McWilliams, J. C. (1990). Isopycnal mixing in ocean circulation models. *Journal of Physical Oceanography*, *20*(1), 150–155.

Gentine, P., Pritchard, M., Rasp, S., Reinaudi, G., & Yacalis, G. (2018). Could machine learning break the convection parameterization deadlock? <https://agupubs.onlinelibrary.wiley.com/doi/10.1029/2018GL078202>. *Geophysical Research Letters*, *45*(11), 5742–5751.

Gettelman, A., Hannay, C., Bacmeister, J. T., Neale, R. B., Pendergrass, A. G., Danabasoglu, G., Lamarque, J. F., Fasullo, J. T., Bailey, D. A., Lawrence, D. M., & Mills, M. J. (2019). High climate sensitivity in the Community Earth System Model Version 2 (CESM2) <https://doi.org/10.1029/2019GL083978>. *Geophysical Research Letters*, *46*(14), 8329–8337.

Gettelman, A., Mills, M. J., Kinnison, D. E., Garcia, R. R., Smith, A. K., Marsh, D. R., Tilmes, S., Vitt, F., Bardeen, C. G., McInerny, J., Liu, H. L., Solomon, S. C., Polvani, L. M., Emmons, L. K., Lamarque, J. F., Richter, J. H., Glanville, A. S., Bacmeister, J. T., Phillips, A. S., . . . Randel, W. J. (2019). The Whole Atmosphere Community Climate Model Version 6 (WACCM6) <https://doi.org/10.1029/2019JD030943>. *Journal of Geophysical Research: Atmospheres*, *124*(23), 12380–12403.

Gettelman, A., Truesdale, J. E., Bacmeister, J. T., Caldwell, P. M., Neale, R. B., Bogenschutz, P. A., & Simpson, I. R. (2019). The Single Column Atmosphere Model Version 6 (SCAM6): Not a scam but a tool for model evaluation and development <https://doi.org/10.1029/2018MS001578>. *Journal of Advances in Modeling Earth Systems*, *11*(5), 1381–1401.

Ginu-Bogdan, A., Hourdin, F., Traore, A. K., & Braconnot, P. (2018). Omens of coupled model biases in the CMIP5 AMIP simulations <https://doi.org/10.1007/s00382-017-4057-3>. *Climate Dynamics*, *51*(7–8), 2927–2941.

Giorgetta, M. A., Brokopf, R., Crueger, T., Esch, M., Fiedler, S., Helmert, J., Hohenegger, C., Kornblueh, L., Köhler, M., Manzini, E., Mauritsen, T., Nam, C., Raddatz, T., Rast, S., Reinert, D., Sakradzija, M., Schmidt, H., Schneck, R., Schnur, R., . . . Stevens, B. (2018). ICON-A, the atmosphere component of the ICON Earth system model: I. Model description <https://doi.org/10.1029/2017MS001242>. *Journal of Advances in Modeling Earth Systems*, *10*(7), 1613–1637.

Golaz, J. C., Larson, V. E., & Cotton, W. R. (2002). A PDF-based model for boundary layer clouds. Part I: Method and model description <https://journals.ametsoc.org/view/journals/atsc/59/24/1520-0469_2002_059_3540_apbmfb_2.0.co_2.xml>. *Journal of the Atmospheric Sciences*, *59*(24), 3540–3551.

Grabowski, W. W. (2001). Coupling cloud processes with the large-scale dynamics using the Clouds-Resolving Convection Parameterization (CRCP) <https://journals.ametsoc.org/view/journals/atsc/58/9/1520-0469_2001_058_0978_ccpwtl_2.0.co_2.xml>. *Journal of the Atmospheric Sciences*, *58*(9), 978–997.

Gregory, D., & Rowntree, P. R. (1990). A mass flux convection scheme with representation of cloud ensemble characteristics and stability-dependent closure. *Monthly Weather Review*, *118*, 1483–1506.

Griffies, S. M., Winton, M., Anderson, W. G., Benson, R., Del-Worth, T. L., Dufour, C. O., Dunne, J. P., Goddard, P., Morrison, A. K., Rosati, A., Wittenberg, A. T., Yin, J.-J., & Zhang, R. (2015). Impacts on ocean heat from transient mesoscale eddies in a hierarchy of climate models. *Journal of Climate*, *28*(3), 952–977.

Guo, H., Golaz, J. C., Donner, L. J., Wyman, B., Zhao, M., & Ginoux, P. (2015). CLUBB as a unified cloud parameterization: Opportunities and challenges <https://doi.org/10.1002/2015GL063672>. *Geophysical Research Letters*, *42*(11), 4540–4547.

Haarsma, R. J., Roberts, M. J., Vidale, P. L., Senior, C. A., Bellucci, A., Bao, Q., Chang, P., Corti, S., Fučkar, N. S., Guemas, V., von Hardenberg, J., Hazeleger, W., Kodama, C., Koenigk, T., Leung, L. R., Lu, J., Luo, J.-J., Mao, J., Mizielinski, M. S., . . . von Storch, J.-S. (2016). High Resolution Model Intercomparison Project (HighResMIP v1.0) for CMIP6 <https://doi.org/10.5194/gmd-9-4185-2016>. *Geoscientific Model Development*, *9*(11), 4185–4208.

Hallberg, R. (2013). Using a resolution function to regulate parameterizations of oceanic mesoscale eddy effects. *Ocean Modelling*, *72*, 92–103.

Ham, Y. G., Kim, J. H., & Luo, J. J. (2019). Deep learning for multi-year ENSO forecasts <http://dx.doi.org/10.1038/s41586-019-1559-7>. *Nature, 573*(7775), 568–572.

Han, J., Wang, W., Kwon, Y. C., Hong, S.-Y., Tallapragada, V., & Yang, F. (2017). Updates in the NCEP GFS cumulus convection schemes with scale and aerosol awareness <https://doi.org/10.1175/waf-d-17-0046.1>. *Weather and Forecasting*, *32*(5), 2005–2017.

Hannay, C., Williamson, D. L., Hack, J. J., Kiehl, J. T., Olson, J. G., Klein, S. A., Bretherton, C. S., & Köhler, M. (2009). Evaluation of forecasted southeast Pacific stratocumulus in the NCAR, GFDL, and ECMWF models <https://doi.org/10.1175/2008JCLI2479.1>. *Journal of Climate*, *22*(11), 2871–2889.

Hewitt, H. T., Roberts, M., Mathiot, P., Biastoch, A., Blockley, E., Chassignet, E. P., Fox-Kemper, B., Hyder, P., Marshall, D. P., Popova, E., Treguier, A.-M., Zanna, L., Yool, A., Yongqiang, Y., Beadling, R., Bell, M., Kuhlbrodt, T., Arsouze, T., Bellucci, A., . . . Zhang, Q. (2020). Resolving and parameterising the ocean mesoscale in Earth system models <https://link.springer.com/article/10.1007/s40641-020-00164-w>. *Current Climate Change Reports*, *6*, 137–152.

Hobbs, P. V., Matejka, T. J., Herzegh, P. H., Locatelli, J. D., & Houze, R. A. (1980). The mesoscale and microscale structure and organization of clouds and precipitation in midlatitude cyclones. I: A case study of a cold front. *Journal of the Atmospheric Sciences*, *37*, 568–596.

Holloway, C. E., Petch, J. C., Beare, R. J., Bechtold, P., Craig, G. C., Derbyshire, S. H., Donner, L. J., Field, P. R., Gray, S. L., Marsham, J. H., Parker, D. J., Plant, R. S., Roberts, N. M., Schultz, D. M., Stirling, A. J., & Woolnough, S. J. (2014). Understanding and representing atmospheric convection across scales: Recommendations from the meeting held at Dartington Hall, Devon, UK, 28–30 January 2013 <https://doi.org/10.1002/asl2.508>. *Atmospheric Science Letters*, *15*(4), 348–353.

Holloway, C. E., Woolnough, S. J., & Lister, G. M. S. (2012). Precipitation distributions for explicit versus parametrized convection in a large-domain high-resolution tropical case study <https://doi.org/10.1002/qj.1903>. *Quarterly Journal of the Royal Meteorological Society*, *138*(668), 1692–1708.

Holtslag, A. A. M., & Boville, B. A. (1993). Local versus nonlocal boundary-layer diffusion in a global climate model. *Journal of Climate*, *6*, 1825–1842.

Holtslag, A. A. M., Svensson, G., Baas, P., Basu, S., Beare, B., Beljaars, A. C. M., Bosveld, F. C., Cuxart, J., Lindvall, J., Steeneveld, G. J., Tjernström, M., & Van De Wiel, B. J. H. (2013). Stable atmospheric boundary layers and diurnal cycles: Challenges for weather and climate models <https://doi.org/10.1175/BAMS-D-11-00187.1>. *Bulletin of the American Meteorological Society*, *94*(11), 1691–1706.

Holtslag, B. (2006). Preface: GEWEX Atmospheric Boundary-layer Study (GABLS) on stable boundary layers <https://doi.org/10.1007/s10546-005-9008-6>. *Boundary-Layer Meteorology*, *118*(2), 243–246.

Honnert, R., Efstathiou, G. A., Beare, R. J., Ito, J., Lock, A., Neggers, R., Plant, R. S., Shin, H. H., Tomassini, L., & Zhou, B. (2020). The atmospheric boundary layer and the Gray zone of turbulence: A critical review <https://doi.org/10.1029/2019JD030317>. *Journal of Geophysical Research: Atmospheres*, *125*(13), 1–26.

Hourdin, F., Jam, A., Rio, C., Couvreux, F., Sandu, I., Lefebvre, M. P., Brient, F., & Idelkadi, A. (2019). Unified parameterization of convective boundary layer transport and clouds with the thermal plume model <https://doi.org/10.1029/2019MS001666>. *Journal of Advances in Modeling Earth Systems*, *11*(9), 2910–2933.

Hourdin, F., Mauritsen, T., Gettelman, A., Golaz, J. C., Balaji, V., Duan, Q., Folini, D., Ji, D., Klocke, D., Qian, Y., Rauser, F., Rio, C., Tomassini, L., Watanabe, M., & Williamson, D. (2017). The art and science of climate model tuning <https://doi.org/10.1175/BAMS-D-15-00135.1>. *Bulletin of the American Meteorological Society*, *98*(3), 589–602.

Hourdin, F., Rio, C., Grandpeix, J. Y., Madeleine, J. B., Cheruy, F., Rochetin, N., Jam, A., Musat, I., Idelkadi, A., Fairhead, L., Foujols, M. A., Mellul, L., Traore, A. K., Dufresne, J. L., Boucher, O., Lefebvre, M. P., Millour, E., Vignon, E., Jouhaud, J., . . . Ghattas, J. (2020). LMDZ6A: The atmospheric component of the IPSL climate model with improved and better tuned physics <https://doi.org/10.1029/2019MS001892>. *Journal of Advances in Modeling Earth Systems*, *12*(7), 1–37.

Hourdin, F., Williamson, D., Rio, C., Couvreux, F., Roehrig, R., Villefranque, N., Musat, I., Fairhead, L., Diallo, F. B., & Volodina, V. (2021). Process-based climate model development harnessing machine learning: II. Model calibration from single column to global <https://doi.org/10.1029/2020MS002225>. *Journal of Advances in Modeling Earth Systems*, *13*(6), e2020MS002225.

Huber, M. B., & Zanna, L. (2017). Drivers of uncertainty in simulated ocean circulation and heat uptake. *Geophysical Research Letters*, *44*(3), 1402–1413.

Hurrell, J., Meehl, G. A., Bader, D., Delworth, T. L., Kirtman, B., & Wielicki, B. (2009). A unified modeling approach to climate system prediction <https://doi.org/10.1175/2009BAMS2752.1>. *Bulletin of the American Meteorological Society*, *90*(12), 1819–1832.

Hyder, P., Edwards, J. M., Allan, R. P., Hewitt, H. T., Bracegirdle, T. J., Gregory, J. M., Wood, R. A., Meijers, A. J. S., Mulcahy, J., Field, P., Furtado, K., Bodas-Salcedo, A., Williams, K. D., Copsey, D., Josey, S. A., Liu, C., Roberts, C. D., Sanchez, C., Ridley, J., . . . Belcher, S. E. (2018). Critical Southern Ocean climate model biases traced to atmospheric model cloud errors <https://doi.org/10.1038/s41467-018-05634-2>. *Nature Communications*, *9*(1), Article 3625.

Iacono, M. J., Mlawer, E. J., Clough, S. A., & Morcrette, J. J. (2000). Impact of an improved longwave radiation model, RRTM, on the energy budget and thermodynamic properties of the NCAR community climate model, CCM3 <https://doi.org/10.1029/2000JD900091>. *Journal of Geophysical Research Atmospheres*, *105*(D11), 14873–14890.

Jansen, M. F., & Held, I. M. (2014). Parameterizing subgrid-scale eddy effects using energetically consistent backscatter. *Ocean Modelling*, *80*, 36–48.

Juricke, S., Palmer, T. N., & Zanna, L. (2017). Stochastic subgrid-scale ocean mixing: Impacts on low-frequency variability <https://doi.org/10.1175/JCLI-D-16-0539.1>. *Journal of Climate*, *30*(13), 4997–5019.

Kain, J. S. (2004). The Kain–Fritsch convective parameterization: An update. *Journal of Applied Meteorology*, *43*(1), 170–181.

Khain, A. P., Beheng, K. D., Heymsfield, A., Korolev, A., Krichak, S. O., Levin, Z., Pinsky, M., Phillips, V., Prabhakaran, T., Teller, A., van den, S. C., & Yano, J.-I. (2015). Representation of microphysical processes in cloudresolving models: Spectral (bin) microphysics versus bulk parameterization. *Reviews of Geophysics*, *53*, 247–322.

Khairoutdinov, M. F., Randall, D., & DeMott, C. (2005). Simulations of the atmospheric general circulation using a cloud-resolving model as a superparameterization of physical processes. *Journal of the Atmospheric Sciences*, *62*, 2136–2154.

Khairoutdinov, M. F., & Randall, D. A. (2001). A cloud resolving model as a cloud parameterization in the NCAR community climate system model: Preliminary results <https://doi.org/10.1029/2001GL013552>. *Geophysical Research Letters*, *28*(18), 3617–3620.

Kirtman, B. P., Bitz, C., Bryan, F., Collins, W., Dennis, J., Hearn, N., Kinter, J. L., Loft, R., Rousset, C., Siqueira, L., Stan, C., Tomas, R., & Vertenstein, M. (2012). Impact of ocean model resolution on CCSM climate simulations. *Climate Dynamics*, *39*(6), 1303–1328.

Klinger, B. A., Marshall, J., & Send, U. (1996). Representation of convective plumes by vertical adjustment. *Journal of Geophysical Research: Oceans*, *101*(C8), 18175–18182.

Klinker, E., & Sardeshmukh, P. D. (1992). The diagnosis of mechanical dissipation in the atmosphere from large-scale balance requirements. *Journal of the Atmospheric Sciences*, *49*(7), 608–627.

Knight, C. G., Knight, S. H. E., Massey, N., Aina, T., Christensen, C., Frame, D. J., Kettleborough, J. A., Martin, A., Pascoe, S., Sanderson, B., Stainforth, D. A., & Allen, M. R. (2007). Association of parameter, software, and hardware variation with large-scale behavior across 57,000 climate models <https://doi.org/10.1073/pnas.0608144104>. *Proceedings of the National Academy of Sciences of the USA*, *104*(30), 12259–12264.

Kooperman, G. J., Pritchard, M. S., Burt, M. A., Branson, M. D., & Randall, D. A. (2016). Impacts of cloud superparameterization on projected daily rainfall intensity climate changes in multiple versions of the Community Earth System Model <https://doi.org/10.1002/2016MS000715>. *Journal of Advances in Modeling Earth Systems*, *8*, 1727–1750.

Krasnopolsky, V. M., Fox-Rabinovitz, M. S., & Chalikov, D. V. (2005). New approach to calculation of atmospheric model physics: Accurate and fast neural network emulation of longwave radiation in a climate model. *Monthly Weather Review*, *133*(12), 3721–3723.

Kuang, Z., & Bretherton, C. S. (2006). A mass-flux scheme view of a high-resolution simulation of a transition from shallow to deep cumulus convection <https://doi.org/10.1175/JAS3723.1>. *Journal of the Atmospheric Sciences*, *63*(7), 1895–1909.

Large, W. G., McWilliams, J. C., & Doney, S. C. (1994). Oceanic vertical mixing: A review and a model with a nonlocal boundary layer parameterization. *Reviews of Geophysics*, *32*(4), 363–403.

Lazarevich, P., Rossby, T., & McNeil, C. (2004). Oxygen variability in the near-surface waters of the northern North Atlantic: Observations and a model <https://doi.org/10.1357/0022240042387547>. *Journal of Marine Research*, *62*(5), 663–683.

Leith, C. E. (1968). Diffusion approximation for two-dimensional turbulence. *The Physics of Fluids*, *11*(3), 671–672.

Leutbecher, M., Lock, S. J., Ollinaho, P., Lang, S. T. K., Balsamo, G., Bechtold, P., Bonavita, M., Christensen, H. M., Diamantakis, M., Dutra, E., English, S., Fisher, M., Forbes, R. M., Goddard, J., Haiden, T., Hogan, R. J., Juricke, S., Lawrence, H., MacLeod, D., . . . Weisheimer, A. (2017). Stochastic representations of model uncertainties at ECMWF: State of the art and future vision <https://doi.org/10.1002/qj.3094>. *Quarterly Journal of the Royal Meteorological Society*, *143*(707), 2315–2339.

Lilly, D. K. (1968). Models of cloud-topped mixed layers under a strong inversion <https://doi.org/10.1002/qj.49709440106>. *Quarterly Journal of the Royal Meteorological Society*, *94*(401), 292–309.

Lin, Y. L., Farley, R. D., & Orville, H. D. (1983). Bulk parameterization of the snow field in a cloud model. *Journal of Climate & Applied Meteorology*, *22*(6), 1065–1092.

Ling, J., Jones, R., & Templeton, J. (2016). Machine learning strategies for systems with invariance properties. *Journal of Computational Physics*, *318*, 22–35.

Lovejoy, S., & Schertzer, D. (2013). *The weather and climate: Emergent laws and multifractal cascades*. Cambridge University Press.

Lynch, P. (2006). *The emergence of numerical weather prediction: Richardson's dream*. Cambridge University Press.

Machenhauer, B., Kaas, E., & Lauritzen, P. H. (2009). Finite-volume methods in meteorology. In R. Tenan & J. Tribbia (Eds.), *Computational methods for the atmosphere and oceans* (pp. 3–120). Elsevier.

MacKinnon, J. A., Alford, M. H., Ansong, J. K., Arbic, B. K., Barna, A., Briegleb, B. P., Bryan, F. O., Buijsman, M. C., Chassignet, E. P., Danabasoglu, G., Diggs, S., Griffies, S. M., Hallberg, R. W., Jayne, S. R., Jochum, M., Klymak, J. M., Kunze, E., Large, W. G., Legg, S., . . . Zhao, Z. (2017). Climate process team on internal wave–driven ocean mixing. *Bulletin of the American Meteorological Society*, *98*(11), 2429–2454.

Manabe, S., Smagorinsky, J., & Strickler, R. F. (1965). Simulated climatology of a general circulation model with a hydrologic cycle. *Monthly Weather Review*, *93*, 769–798.

Marshall, D. P., & Adcroft, A. J. (2010). Parameterization of ocean eddies: Potential vorticity mixing, energetics and Arnold's first stability theorem. *Ocean Modelling*, *32*(3–4), 188–204.

Marshall, D. P., Maddison, J. R., & Berloff, P. S. (2012). A framework for parameterizing eddy potential vorticity fluxes. *Journal of Physical Oceanography*, *42*(4), 539–557.

Martin, G. M., Milton, S. F., Senior, C. A., Brooks, M. E., Ineson, S., Reichler, T., & Kim, J. (2010). Analysis and reduction of systematic errors through a seamless approach to modeling weather and climate *<https://doi.org/10.1175/2010JCLI3541.1>*. *Journal of Climate*, *23*(22), 5933–5957.

Maulik, R., & San, O. (2017). A neural network approach for the blind deconvolution of turbulent flows. *Journal of Fluid Mechanics*, *831*, 151–181.

Maulik, R., San, O., Jacob, J. D., & Crick, C. (2019). Sub-grid scale model classification and blending through deep learning *<https://doi.org/10.1017/jfm.2019.254>*. *Journal of Fluid Mechanics*, *870*, 784–812.

Medeiros, B., Williamson, D. L., Hannay, C., & Olson, J. G. (2012). Southeast Pacific stratocumulus in the community atmosphere model *<https://doi.org/10.1175/JCLI-D-11-00503.1>*. *Journal of Climate*, *25*(18), 6175–6192.

Moeng, C.-H. (2016). *Lecture notes on the planetary boundary layer* *<https://doi.org/10.5065/D6891467>* (Technical report NCAR/TN-525+IA). National Center for Atmospheric Research.

Moncrieff, M. W. (2019). Toward a dynamical foundation for organized convection parameterization in GCMs *<https://doi.org/10.1029/2019GL085316>*. *Geophysical Research Letters*, *46*(23), 14103–14108.

Moncrieff, M. W., Liu, C., & Bogenschutz, P. (2017). Simulation, modeling, and dynamically based parameterization of organized tropical convection for global climate models *<https://doi.org/10.1175/JAS-D-16-0166.1>*. *Journal of the Atmospheric Sciences*, *74*(5), 1363–1380.

Monin, A. S., & Obukhov, A. M. (1954). Osnovnye zakonomernosti turbulentnogo pere- meshivanija v prizemnom sloe atmosfery (Basic laws of turbulent mixing in the atmosphere near the ground). *Trudy Geofizicheskogo Instituta, Akademiya Nauk SSSR*, *24*(151), 163–187.

Morcrette, J. J., Barker, H. W., Cole, J. N. S., Iacono, M. J., & Pincus, R. (2008). Impact of a new radiation package, McRad, in the ECMWF integrated forecasting system *<https://doi.org/10.1175/2008MWR2363.1>*. *Monthly Weather Review*, *136*(12), 4773–4798.

Morcrette, J. J., Mozdzynski, G., & Leutbecher, M. (2008). A reduced radiation grid for the ECMWF integrated forecasting system *<https://doi.org/10.1175/2008MWR2590.1>*. *Monthly Weather Review*, *136*(12), 4760–4772.

Morrison, H., Thompson, G., & Tatarskii, V. (2009). Impact of cloud microphysics on the development of trailing stratiform precipitation in a simulated squall line: Comparison of one- and two-moment schemes <https://doi.org/10.1175/2008MWR2556.1>. *Monthly Weather Review*, *137*(3), 991–1007.

Murakami, M. (1990). Numerical modeling of dynamical and micro-physical evolution of an isolated convective cloud. The 19 July 1981 CCOPE cloud. *Journal of the Meteorological Society of Japan*, *68*, 107–128.

Nastrom, G. D., & Gage, K. S. (1985). A climatology of atmospheric wavenumber spectra of wind and temperature observed by commercial aircraft. *Journal of the Atmospheric Sciences*, *42*(9), 950–960.

O'Brien, J. J. (1970). A note on the vertical structure of the eddy exchange coefficient in the planetary boundary layer. *Journal of the Atmospheric Sciences*, *27*(8), 1213–1215.

O'Gorman, P. A., & Dwyer, J. G. (2018). Using machine learning to parameterize moist convection: Potential for modeling of climate, climate change, and extreme events <https://doi.org/10.1029/2018MS001351>. *Journal of Advances in Modeling Earth Systems*, *10*(10), 2548–2563.

Ollinaho, P., Lock, S.-J., Leutbecher, M., Bechtold, P., Beljaars, A., Bozzo, A., Forbes, R. M., Haiden, T., Hogan, R. J., & Sandu, I. (2017). Towards process-level representation of model uncertainties: Stochastically perturbed parametrizations in the ECMWF ensemble. *Quarterly Journal of the Royal Meteorological Society*, *143*(702), 408–422.

Palmer, T. N., Doblas-Reyes, F. J., Weisheimer, A., & Rodwell, M. J. (2008). Towards seamless prediction: Calibration of climate change projections using seasonal forecasts. *Bulletin of the American Meteorological Society*, *89*(4), 459–470.

Palmer, T. N., & Weisheimer, A. (2011). Diagnosing the causes of bias in climate models—Why is it so hard? <https://doi.org/10.1080/03091929.2010.547194>. *Geophysical and Astrophysical Fluid Dynamics*, *105*(2–3), 351–365.

Pearson, K. J., Lister, G. M. S., Birch, C. E., Allan, R. P., Hogan, R. J., & Woolnough, S. J. (2014). Modelling the diurnal cycle of tropical convection across the "grey zone" <https://doi.org/10.1002/qj.2145>. *Quarterly Journal of the Royal Meteorological Society*, *140*(679), 491–499.

Petch, J. C., Willett, M., Wong, R. Y., & Woolnough, S. J. (2007). Modelling suppressed and active convection. Comparing a numerical weather prediction, cloud-resolving and single-column model. *Quarterly Journal of the Royal Meteorological Society*, *133*(626 A), 1087–1100.

Phillips, T. J., Potter, G. L., Williamson, D. L., Cederwall, R. T., Boyle, J. S., Fiorino, M., Hnilo, J. J., Olson, J. G., Xie, S., & Yio, J. J. (2004). Evaluating parameterizations in general circulation models: Climate simulation meets weather prediction <https://doi.org/10.1175/BAMS-85-12-1903>. *Bulletin of the American Meteorological Society*, *85*(12), 1903–1915.

Pincus, R., Barker, H. W., & Morcrette, J. J. (2003). A fast, flexible, approximate technique for computing radiative transfer in inhomogeneous cloud fields <https://doi.org/10.1029/2002jd003322>. *Journal of Geophysical Research D: Atmospheres*, *108*(13).

Pincus, R., & Stevens, B. (2013). Paths to accuracy for radiation parameterizations in atmospheric models <https://doi.org/10.1002/jame.20027>. *Journal of Advances in Modeling Earth Systems*, *5*(2), 225–233.

Plant, R. S. (2010). A review of the theoretical basis for bulk mass flux convective parameterization <https://doi.org/10.5194/acp-10-3529-2010>. *Atmospheric Chemistry and Physics*, *10*(8), 3529–3544.

Plant, R. S., & Craig, G. C. (2008). A stochastic parameterization for deep convection based on equilibrium statistics <https://doi.org/10.1175/2007JAS2263.1>. *Journal of the Atmospheric Sciences*, *65*(1), 87–105.

Plant, R. S., & Yano, J.-I. (2016). *Parameterization of atmospheric convection (in two volumes)*. Imperial College Press.

Porta Mana, P., & Zanna, L. (2014). Toward a stochastic parameterization of ocean mesoscale eddies <https://doi.org/10.1016/j.ocemod.2014.04.002>. *Ocean Modelling*, *79*, 1–20.

Price, J. F., Weller, R. A., & Pinkel, R. (1986). Diurnal cycling: Observations and models of the upper ocean response to diurnal heating, cooling, and wind mixing <https://doi.org/10.1029/jc091ic07p08411>. *Journal of Geophysical Research: Oceans*, *91*(6), 8411–8427.

Pritchard, M. S., Bretherton, C. S., & DeMott, C. A. (2014). Restricting 32–128 km horizontal scales hardly affects the MJO in the Superparameterized Community Atmosphere Model v.3.0 but the number of cloud-resolving grid columns constrains vertical mixing <https://doi.org/10.1002/2014MS000340>. *Journal of Advances in Modeling Earth Systems*, *6*, 723–739.

Pritchard, M. S., Moncrieff, M. W., & Somerville, R. C. J. (2011). Orogenic propagating precipitation systems over the United States in a global climate model with embedded explicit convection <https://doi.org/10.1175/2011JAS3699.1>. *Journal of the Atmospheric Sciences*, *68*(8), 1821–1840.

Qin, H., Pritchard, M. S., Kooperman, G. J., & Parishani, H. (2018). Global effects of superparameterization on hydrothermal land–atmosphere coupling on multiple timescales <https://doi.org/10.1002/2017MS001185>. *Journal of Advances in Modeling Earth Systems*, *10*(2), 530–549.

Rackow, T., & Juricke, S. (2020). Flow-dependent stochastic coupling for climate models with high ocean-to-atmosphere resolution ratio. *Quarterly Journal of the Royal Meteorological Society*, *146*(726), 284–300.

Randall, D. A., Xu, K.-M., Somerville, R. J. C., & Iacobellis, S. (1996). Single-column models and cloud ensemble models as links between observations and climate models <https://journals.ametsoc.org/view/journals/clim/9/8/1520-0442_1996_009_1683_scmace_2_0_co_2.xml>. *Journal of Climate*, *9*(8), 1683–1697.

Rasmusson, E. M., & Wallace, J. M. (1983). Meteorological aspects of the El Nino/Southern Oscillation <https://doi.org/10.1126/science.222.4629.1195>. *Science*, *222*(4629), 1195–1202.

Redi, M. H. (1982). Oceanic isopycnal mixing by coordinate rotation. *Journal of Physical Oceanography*, *12*(10), 1154–1158.

Rodwell, M. J., Lang, S. T. K., Ingleby, B., Bormann, N., Hólm, E., Rabier, F., Richardson, D. S., & Yamaguchi, M. (2016). Reliability in ensemble data assimilation. *Quarterly Journal of the Royal Meteorological Society*, *142*(694), 443–454.

Rodwell, M. J., & Palmer, T. N. (2007). Using numerical weather prediction to assess climate models. *Quarterly Journal of the Royal Meteorological Society*, *133*(622), 129–146.

Rodwell, M. J., Richardson, D. S., Parsons, D. B., & Wernli, H. (2018, May). Flow-dependent reliability: A path to more skillful ensemble forecasts <https://doi.org/10.1175/BAMS-D-17-0027.1>. *Bulletin of the American Meteorological Society*, *99*(5), 1015–1026.

Salehipour, H., & Peltier, W. R. (2019). Deep learning of mixing by two atoms of stratified turbulence. *Journal of Fluid Mechanics*, *861*, R4.

Sanchez, C., Williams, K. D., & Collins, M. (2016). Improved stochastic physics schemes for global weather and climate models. *Quarterly Journal of the Royal Meteorological Society*, *142*(694), 147–159.

Sasaki, H., Klein, P., Qiu, B., & Sasai, Y. (2014). Impact of oceanic-scale interactions on the seasonal modulation of ocean dynamics by the atmosphere *<https://doi.org/10.1038/ncomms6636>*. *Nature Communications*, *5*, Article 5636.

Schalkwijk, J., Jonker, H. J. J., Siebesma, A. P., & Van Meijgaard, E. (2015). Weather forecasting using GPU-based large-eddy simulations *<https://doi.org/10.1175/BAMS-D-14-00114.1>*. *Bulletin of the American Meteorological Society*, *96*(5), 715–723.

Schmidt, G. A., Bader, D., Donner, L. J., Elsaesser, G. S., Golaz, J.-C., Hannay, C., Molod, A., Neale, R. B., & Saha, S. (2017). Practice and philosophy of climate model tuning across six US modeling centers *<https://doi.org/10.5194/gmd-10-3207-2017>*. *Geoscientific Model Development*, *10*, 3207–3223.

Schneider, T., Lan, S., Stuart, A., & Teixeira, J. (2017). Earth System Modeling 2.0: A blueprint for models that learn from observations and targeted high-resolution simulations. *Geophysical Research Letters*, *44*(24), 12–396.

Schneider, T., Teixeira, J., Bretherton, C. S., Brient, F., Pressel, K. G., Schär, C., & Siebesma, A. P. (2017). Climate goals and computing the future of clouds. *Nature Climate Change*, *7*(1), 3–5.

Seidel, D. J., Ao, C. O., & Li, K. (2010). Estimating climatological planetary boundary layer heights from radiosonde observations: Comparison of methods and uncertainty analysis *<https://doi.org/10.1029/2009JD013680>*. *Journal of Geophysical Research Atmospheres*, *115*(16), 1–15.

Shonk, J. K. P., Hogan, R. J., Edwards, J. M., & Mace, G. G. (2010). Effect of improving representation of horizontal and vertical cloud structure on the Earth's global radiation budget. Part I: Review and parametrization *<https://doi.org/10.1002/qj.647>*. *Quarterly Journal of the Royal Meteorological Society*, *136*(650), 1191–1204.

Shutts, G. J., & Palmer, T. N. (2007). Convective forcing fluctuations in a cloud-resolving model: Relevance to the stochastic parameterization problem *<https://doi.org/10.1175/JCLI3954.1>*. *Journal of Climate*, *20*(2), 187–202.

Siebesma, A. P., Soares, P. M. M., & Teixeira, J. (2007). A combined eddy-diffusivity mass-flux approach for the convective boundary layer *<https://doi.org/10.1175/jas3888.1>*. *Journal of the Atmospheric Sciences*, *64*(4), 1230–1248.

Smagorinsky, J. (1963). General circulation experiments with the primitive equations: I. The basic experiment. *Monthly Weather Review*, *91*(3), 99–164.

Steeneveld, G. J. (2014, October). Current challenges in understanding and forecasting stable boundary layers over land and ice *<https://doi.org/10.3389/fenvs.2014.00041>*. *Frontiers in Environmental Science*, *2*, 1–6.

Stensrud, D. J. (2007). *Parameterization schemes: Keys to understanding numerical weather prediction models*. Cambridge University Press.

Stephens, G. (1984). The parameterization of radiation for numerical weather prediction and climate models. *Monthly Weather Review*, *112*, 826–867.

Stevens, B., Acquistapace, C., Hansen, A., Heinze, R., Klinger, C., Klocke, D., Rybka, H., Schubotz, W., Windmiller, J., Adamidis, P., Arka, I., Barlakas, V., Biercamp, J., Brueck, M., Brune, S., Buehler, S. A., Burkhardt, U., Cioni, G., Costa-Surós, M., . . . Zängl, G. (2020). The added value of large-eddy and storm-resolving models for simulating clouds and precipitation <https://doi.org/10.2151/jmsj.2020-021>. *Journal of the Meteorological Society of Japan*, *98*(2), 395–435.

Stevens, B., Satoh, M., Auger, L., Biercamp, J., Bretherton, C. S., Chen, X., Düben, P., Judt, F., Khairoutdinov, M., Klocke, D., Kodama, C., Kornblueh, L., Lin, S. J., Neumann, P., Putman, W. M., Röber, N., Shibuya, R., Vanniere, B., Vidale, P. L., . . . Zhou, L. (2019). DYAMOND: The DYnamics of the Atmospheric general circulation Modeled On Non-hydrostatic Domains <https://doi.org/10.1186/s40645-019-0304-z>. *Progress in Earth and Planetary Science*, *6*(1), Article 61.

Storer, R. L., Griffin, B. M., Höft, J., Weber, J. K., Raut, E., Larson, V. E., Wang, M., & Rasch, P. J. (2015). Parameterizing deep convection using the assumed probability density function method <https://doi.org/10.5194/gmd-8-1-2015>. *Geoscientific Model Development*, *8*(1), 1–19.

Strommen, K., Christensen, H. M., Macleod, D., Juricke, S., & Palmer, T. N. (2019). Progress towards a probabilistic Earth system model: Examining the impact of stochasticity in the atmosphere and land component of EC-Earth v3.2 <https://doi.org/10.5194/gmd-12-3099-2019>. *Geoscientific Model Development*, *12*(7), 3099–3118.

Subel, A., Chattopadhyay, A., Guan, Y., & Hassanzadeh, P. (2021). Data-driven subgrid-scale modeling of forced Burgers turbulence using deep learning with generalization to higher Reynolds numbers via transfer learning. *Physics of Fluids*, *33*(3), 031702.

Sueyoshi, T., Ohgaito, R., Yamamoto, A., Chikamoto, M. O., Hajima, T., Okajima, H., Yoshimori, M., Abe, M., O'ishi, R., Saito, F., Watanabe, S., Kawamiya, M., & Abe-Ouchi, A. (2013). Set-up of the PMIP3 paleoclimate experiments conducted using an Earth system model, MIROC-ESM <https://doi.org/10.5194/gmd-6-819-2013>. *Geoscientific Model Development*, *6*(3), 819–836.

Sušelj, K., Hogan, T. F., & Teixeira, J. (2014). Implementation of a stochastic eddy-diffusivity/mass-flux parameterization into the Navy Global Environmental Model <https://doi.org/10.1175/waf-d-14-00043.1>. *Weather and Forecasting*, *29*(6), 1374–1390.

Sušelj, K., Kurowski, M. J., & Teixeira, J. (2019). A unified eddy-diffusivity/mass-flux approach for modeling atmospheric convection <https://doi.org/10.1175/JAS-D-18-0239.1>. *Journal of the Atmospheric Sciences*, *76*(8), 2505–2537.

Sušelj, K., Teixeira, J., & Chung, D. (2013). A unified model for moist convective boundary layers based on a stochastic eddy-diffusivity/mass-flux parameterization <https://doi.org/10.1175/jas-d-12-0106.1>. *Journal of the Atmospheric Sciences*, *70*(7), 1929–1953.

Tan, I., Storelvmo, T., & Zelinka, M. D. (2016). Observational constraints on mixed-phase clouds imply higher climate sensitivity. *Science*, *352*(6282), 224–227.

Tang, S., Zhang, M., & Xie, S. (2017). Investigating the dependence of SCM simulated precipitation and clouds on the spatial scale of large-scale forcing at SGP. *Journal of Geophysical Research Atmospheres*, *122*(16), 8724–8738.

Tiedtke, M. (1989). A comprehensive mass flux scheme for cumulus parameterization in large scale models. *Monthly Weather Review*, *117*, 1779–1800.

Tréguier, A.-M., Deshayes, J., Lique, C., Dussin, R., & Molines, J.-M. (2012). Eddy contributions to the meridional transport of salt in the North Atlantic <https://doi.org/10.1029/2012JC007927>. *Journal of Geophysical Research: Oceans*, *117*(C5).

van Niekerk, A., Scinocca, J. F., & Shepherd, T. G. (2017). The modulation of stationary waves, and their response to climate change, by parameterized orographic drag. *Journal of the Atmospheric Sciences*, *74*(8), 2557–2574.

Van Roekel, L., Adcroft, A. J., Danabasoglu, G., Griffies, S. M., Kauffman, B., Large, W., Levy, M., Reichl, B. G., Ringler, T., & Schmidt, M. (2018). The KPP boundary layer scheme for the ocean: Revisiting its formulation and benchmarking one-dimensional simulations relative to LES <https://doi.org/10.1029/2018MS001336>. *Journal of Advances in Modeling Earth Systems*, *10*(11), 2647–2685.

Veerman, M. A., Pincus, R., Stoffer, R., van Leeuwen, C. M., Podareanu, D., & van Heerwaarden, C. C. (2021). Predicting atmospheric optical properties for radiative transfer computations using neural networks <https://doi.org/10.1098/rsta.2020.0095>. *Philosophical Transactions of the Royal Society A: Mathematical, Physical and Engineering Sciences*, *379*, 20200095.

Von Engeln, A., & Teixeira, J. (2013). A planetary boundary layer height climatology derived from ECMWF reanalysis data <https://doi.org/10.1175/JCLI-D-12-00385.1>. *Journal of Climate*, *26*(17), 6575–6590.

Walters, D. N., Best, M. J., Bushell, A. C., Copsey, D., Edwards, J. M., Falloon, P. D., Harris, C. M., Lock, A. P., Manners, J. C., Morcrette, C. J., Roberts, M. J., Stratton, R. A., Webster, S., Wilkinson, J. M., Willett, M. R., Boutle, I. A., Earnshaw, P. D., Hill, P. G., MacLachlan, C., . . . Williams, K. D. (2019). The Met Office Unified Model Global Atmosphere 3.0/3.1 and JULES Global Land 3.0/3.1 configurations. *Geoscientific Model Development*, *12*, 919–941.

Wang, Q., Danilov, S., Sidorenko, D., Timmermann, R., Wekerle, C., Wang, X., Jung, T., & Schröter, J. (2014). The Finite Element Sea Ice-Ocean Model (FESOM) v.1.4: Formulation of an ocean general circulation model. *Geoscientific Model Development*, *7*(2), 663–693.

Warner, T. T. (2011). *Numerical weather and climate prediction*. Cambridge University Press.

Weisheimer, A., & Palmer, T. N. (2014). On the reliability of seasonal climate forecasts <https://royalsocietypublishing.org/doi/10.1098/rsif.2013.1162>. *Journal of the Royal Society Interface*, *11*.

Williams, K. D., Bodas-Salcedo, A., Déqué, M., Fermepin, S., Medeiros, B., Watanabe, M., Jakob, C., Klein, S. A., Senior, C. A., & Williamson, D. L. (2013). The transpose-AMIP II experiment and its application to the understanding of Southern Ocean cloud biases in climate models <https://doi.org/10.1175/JCLI-D-12-00429.1>. *Journal of Climate*, *26*(10), 3258–3274.

Williams, K. D., Hewitt, A. J., & Bodas-Salcedo, A. (2020). Use of short-range forecasts to evaluate fast physics processes relevant for climate sensitivity. *Journal of Advances in Modeling Earth Systems*, *12*(4), e2019MS001986.

Williamson, D. L., Olson, J. G., Hannay, C., Toniazzo, T., Taylor, M., & Yudin, V. (2015). Energy considerations in the community atmosphere <https://doi.org/10.1002/2015MS000448>. *Journal of Advances in Modeling Earth Systems*, *7*(3), 1178–1188.

Wyngaard, J. C. (2004). Toward numerical modeling in the "terra incognita." <https://doi.org/10.1175/1520-0469(2004)061%3c1816:TNMITT%3e2.0.CO;2>. *Journal of the Atmospheric Sciences*, *61*(14), 1816–1826.

Xie, B., Fung, J. C. H., Chan, A., & Lau, A. (2012). Evaluation of nonlocal and local planetary boundary layer schemes in the WRF model <https://doi.org/10.1029/2011JD017080>. *Journal of Geophysical Research Atmospheres*, *117*(12).

Yanai, M., Esbensen, S., & Chu, J.-H. (1973). Determination of bulk properties of tropical cloud clusters from large-scale heat and moisture budgets. *Journal of the Atmospheric Sciences*, *30*, 611–627.

Yano, J. I. (2014). Formulation structure of the mass-flux convection parameterization <https://doi.org/10.1016/j.dynatmoce.2014.04.002>. *Dynamics of Atmospheres and Oceans*, *67*, 1–28.

Yuval, J., & O'Gorman, P. A. (2020). Stable machine-learning parameterization of subgrid processes for climate modeling at a range of resolutions <https://doi.org/10.1038/s41467-020-17142-3>. *Nature Communications*, *11*(3295), Article 3295.

Yuval, J., O'Gorman, P. A., & Hill, C. N. (2021). Use of neural networks for stable, accurate and physically consistent parameterization of subgrid atmospheric processes with good performance at reduced precision <https://doi.org/10.1029/2020gl091363>. *Geophysical Research Letters*, *48*(6), e2020GL091363.

Zanna, L., & Bolton, T. (2020). Data-driven equation discovery of ocean mesoscale closures <https://doi.org/10.1029/2020GL088376>. *Geophysical Research Letters*, *47*(17), e2020GL088376.

Zanna, L., Mana, P. G. L. P., Anstey, J., David, T., & Bolton, T. (2017). Scale-aware deterministic and stochastic parametrizations of eddy-mean flow interaction. *Ocean Modelling*, *111*, 66–80.

Zelinka, M. D., Myers, T. A., McCoy, D. T., Po-Chedley, S., Caldwell, P. M., Ceppi, P., Klein, S. A., & Taylor, K. E. (2020). Causes of higher climate sensitivity in CMIP6 models <https://doi.org/10.1029/2019GL085782>. *Geophysical Research Letters*, *47*(1), e2019GL085782.

Zhang, M., Bretherton, C. S., Blossey, P. N., Austin, P. H., Bacmeister, J. T., Bony, S., Brient, F., Cheedela, S. K., Cheng, A., Del, A. D., De Roode, S. R., Endo, S., Franklin, C. N., Golaz, J. C., Hannay, C., Heus, T., Isotta, F. A., Dufresne, J. L., Kang, I. S., . . . Zhao, M. (2013). CGILS: Results from the first phase of an international project to understand the physical mechanisms of low cloud feedbacks in single column models <https://doi.org/10.1002/2013MS000246>. *Journal of Advances in Modeling Earth Systems*, *5*(4), 826–842.

Zhang, M., Somerville, R. C. J., & Xie, S. (2016). The SCM concept and creation of ARM forcing datasets <https://doi.org/10.1175/AMSMONOGRAPHS-D-15-0040.1>. *Meteorological Monographs*, *57*, 24.1–24.12.

Zhao, N., & Nasuno, T. (2020). How does the air–sea coupling frequency affect convection during the MJO passage? <https://doi.org/10.1029/2020MS002058> *Journal of Advances in Modeling Earth Systems*, *12*(4), e2020MS002058.

Appendix

Methodology for Defining Subgrid Scales

Numerical models explicitly distinguish between subgrid and resolved processes. To use high-resolution data to derive data-driven parametrization schemes, this distinction must be artificially introduced. The subgrid scale is defined using a filtering procedure $\overline{(\cdot)}$ that acts to separate the resolved scales ($\overline{c}$; larger than the grid-box size) from the unresolved scales that are to be parametrized. For a given scalar field *c*, the subgrid scales, $c' = c - \overline{c}$ can then be deduced.

Coarse-graining has long been a natural option to separate resolved and unresolved scales (e.g., Christensen, 2020; Yanai et al., 1973). Coarse-graining takes the weighted (W_{ij}) spatial mean over a subset of grid points (N) within a box, $\overline{c} = (1/N)\sum_{ij} W_{ij}c_{ij}$ The size of the coarse-graining box defines the spatial scale of the resolved state $\overline{c}$. In contrast to time averaging (see the section on "Reynolds Averaging"), coarse-graining typically involves averaging in space as opposed to in time. In addition, the starting point for coarse-graining is some high-resolution data that must be decomposed into resolved and "unresolved" components at some lower resolution, as opposed to the continuous equations of motion, as is the case for Reynolds averaging.

Coarse-graining produces a local definition of subgrid, where quantities outside of the coarse-graining box have no effect on the coarse-grained variable $\overline{c}$. This is consistent with the definition of the grid box in finite volume models (see the section on "From Physical Equations to Numerical Models: Resolved Scale Dynamics"). The disadvantage of this method is that the procedure does not commute with spatial derivatives—that is, $(\partial/\partial x)\overline{c} \neq \overline{(\partial c/\partial x)}$ (i.e., it does not respect Reynolds averaging rules). This can lead to artifacts in the coarse-grained data (figure A.1, left). An alternative to coarse-graining is to use a low-pass spatial filter,

$$\overline{c} = \iint_R c(x,y)k(x,y)dxdy \tag{A.1}$$

where $k(x,y)$ is the filter, and the two-dimensional spatial integral is evaluated over the entire domain (Bolton & Zanna, 2019). Spatial filters do commute with spatial derivatives, preserving conservation properties. They are also more consistent with the grid definition used in finite difference and spectral models (see the section "From Physical Equations to Numerical Models: Resolved Scale Dynamics"). A low-pass filter removes high wavenumbers from the signal, resulting in a smoothed field *c*; the smoothing reduces variability at spatial scales smaller than the predefined scale characterizing the filter. Spatial filtering using a Gaussian kernel produces a more nonlocal definition of subgrid because all grid points, irrespective of location, impact the large-scale field $\overline{c}$ through the integral $\overline{c} = \iint_R c(x,y)k(x,y)dxdy$. However, spatial filters, unlike coarse-graining, do not change the underlying grid size. A solution is to combine spatial filtering and coarse-graining. This is shown in the right panel of figure A.1, where the mean, $\overline{c}$, is first defined using a spatial filter before coarse-graining to a new grid size.

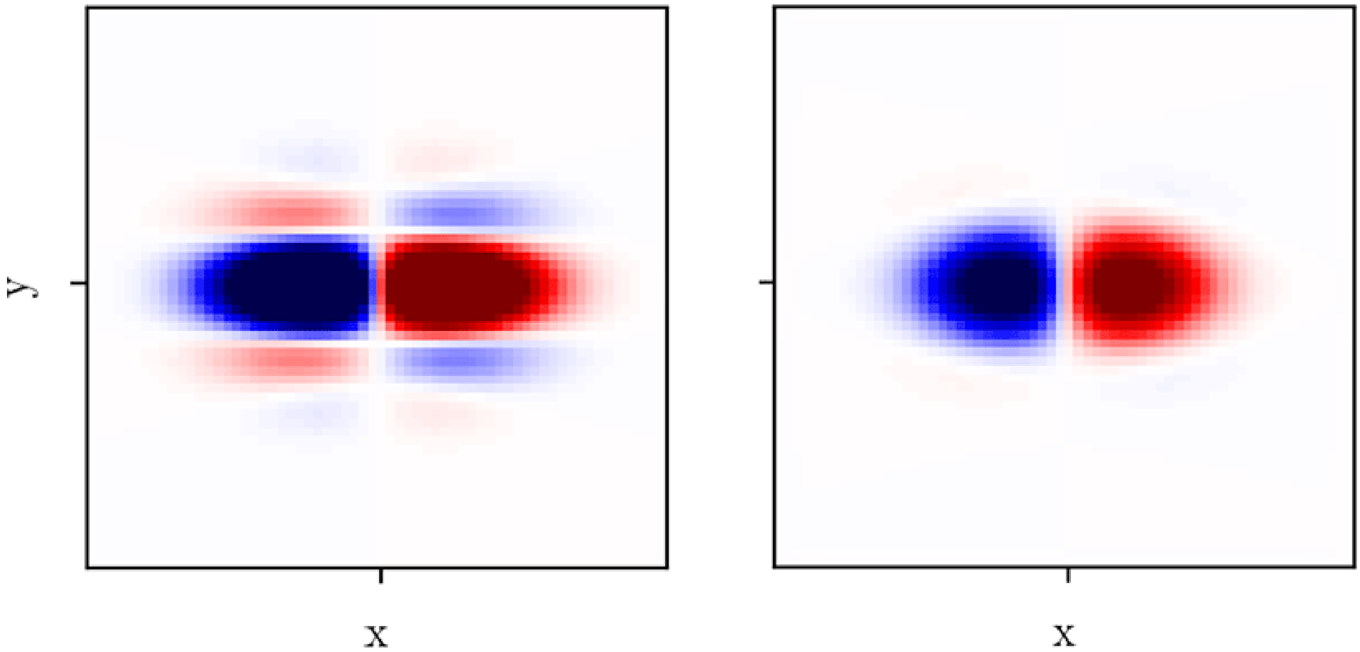

Figure A.1. Illustrations of two averaging procedures using a Gaussian-shaped eddy. Left shows coarse-graining, and right shows spatial filtering and then coarse-graining for the zonal component of the resulting eddy momentum forcing, S_x.

Source: Authors